OPEN ACCESS
IOP Publishing | International Atomic Energy Agency
Nuclear Fusion
Nucl. Fusion **64** (2024) 112006 (25pp)
https://doi.org/10.1088/1741-4326/ad346e

EUROfusion contributions to ITER nuclear operation

X. Litaudon[1,*], U. Fantz[2], R. Villari[3], V. Toigo[4,5], M.-H. Aumeunier[1], J.-L. Autran[6,7], P. Batistoni[3], E. Belonohy[2,8], S. Bradnam[8], M. Cecchetto[9], A. Colangeli[3], F. Dacquait[10], S. Dal Bello[4], M. Dentan[1,9], M. De Pietri[11], J. Eriksson[12], M. Fabbri[13], G. Falchetto[1], L. Figini[5], J. Figueiredo[14,15], D. Flammini[3], N. Fonnesu[3], L. Frassinetti[16], J. Galdón-Quiroga[17], R. Garcia-Alia[9], M. Garcia-Munoz[17], Z. Ghani[8], J. Gonzalez-Martin[18], E. Grelier[1], L. Di Grazia[19], B. Grove[20], C.L. Grove[8], A. Gusarov[21], B. Heinemann[2], A. Hjalmarsson[12], O. Hyvärinen[34], V. Ioannou-Sougleridis[23], L. Jones[8], H.-T. Kim[8], M. Kłosowski[24], M. Kocan[25], B. Kos[20,27], L. Kos[26], D. Kotnik[27,28], E. Laszynska[29], D. Leichtle[30], I. Lengar[27], E. Leon-Gutierrez[31], A.J. López-Revelles[11], S. Loreti[3], M. Loughlin[20], D. Marcuzzi[4], K.G. Mcclements[8], G. Mariano[3], M. Mattei[19], K. Mergia[23], J. Mietelski[24], R. Mitteau[1], S. Moindjie[7], D. Munteanu[7], R. Naish[8], S. Noce[3], L.W. Packer[8], S. Pamela[8], R. Pampin[13], A. Pau[32], A. Peacock[8], E. Peluso[33], Y. Peneliau[1], J. Peric[27,28], V. Radulović[27], D. Ricci[5], F. Rimini[8], L. Sanchis-Sanchez[17], P. Sauvan[11], M.I. Savva[23], G. Serianni[4,5], C.R. Shand[8], A. Snicker[22,34], L. Snoj[27,28], I.E. Stamatelatos[23], Ž. Štancar[8], N. Terranova[3], T. Vasilopoulou[23], R. Vila[31], J. Waterhouse[8], C. Wimmer[2], D. Wünderlich[2], A. Žohar[26], the NBTF Team[a], JET Contributors[b] and the EUROfusion Tokamak Exploitation Team[c]

[1] CEA, IRFM, F-13108 St-Paul-Lez-Durance, France
[2] Max-Planck-Institut für Plasmaphysik, D-85748 Garching, Germany
[3] ENEA, FSN Department, Via E. Fermi 45, 00044 Frascati, Rome, Italy
[4] Consorzio RFX, Corso Stati Uniti 4, I–35127 Padova, Italy
[5] Istituto per la Scienza e Tecnologia dei Plasmi, CNR, Milan, Italy
[6] University of Rennes, CNRS, IPR (UMR 6251), Rennes Cedex, 35 042, France
[7] Aix-Marseille Univ, CNRS, Université de Toulon, IM2NP (UMR 7334), 13397 Marseille Cedex, France
[8] UKAEA, Culham Campus, Abingdon, OX14 3DB, United Kingdom of Great Britain and Northern Ireland
[9] CERN, CH-1211, Geneve 23, Switzerland
[10] CEA, DES, IRESNE, DTN, F-13108 Saint-Paul Lez Durance, France
[11] Departamento de Ingeniería Energética, UNED, Madrid, Spain
[12] Department of Physics and Astronomy, Uppsala University, Uppsala SE-751 20, Sweden
[13] Fusion for Energy (F4E), Josep Pla 2, Torres Diagonal Litoral B3, 08019 Barcelona, Spain
[14] EUROfusion Programme Management Unit, Boltzmannstr. 2, 85748 Garching, Germany
[15] Instituto de Plasmas e Fusão Nuclear, Instituto Superior Técnico, Universidade de Lisboa, Lisboa, Portugal
[16] Division of Electromagnetic Engineering and Fusion Science, KTH, Stockholm, Sweden
[17] Department of Atomic, Molecular and Nuclear Physics, University of Seville, 41012 Seville, Spain
[18] Department of Mechanical Engineering and Manufacturing, University of Seville, 41012 Seville, Spain

[a] See the author list of D. Marcuzzi *et al* 2023 *Fusion Eng. Des.* **191** 113590.
[b] See Maggi *et al* 2024 (https://doi.org/10.1088/1741-4326/ad3e16) for JET Contributors.
[c] See the author list of 'Progress on an exhaust solution for a reactor using EUROfusion multi-machines capabilities' by E. Joffrin *et al* to be published in Nuclear Fusion Special Issue: Overview and Summary Papers from *the 29th Fusion Energy Conference* (*London, UK, 16–21 October 2023*).
* Author to whom any correspondence should be addressed.

[19] Dipartimento di Ingegneria Elettrica e delle Tecnologie dell Informazione, Università degli Studi di Napoli Federico II and with Consorzio CREATE, Napoli, Italy
[20] Oak Ridge National Laboratory, 1 Bethel Valley Road, Oak Ridge, TN, United States of America
[21] SCK CEN, Boeretang 200, B-2400 Mol, Belgium
[22] VTT Technical Research Centre of Finland Ltd, PO Box 1000, Espoo FIN-02044 VTT, Finland
[23] National Centre for Scientific Research 'Demokritos', Athens 15310, Greece
[24] Institute of Nuclear Physics, Polish Academy of Sciences, PL-31-342 Krakow, Poland
[25] ITER Organization, Route de Vinon sur Verdon, CS 90 046, 13067 Saint-Paul-lez-Durance, France
[26] Faculty of Mechanical Engineering, University of Ljubljana, Aškerčeva 6 1000 Ljubljana, Slovenia
[27] Reactor Physics Department, Jožef Stefan Institute, Jamova cesta 39, SI-1000 Ljubljana, Slovenia
[28] Faculty of Mathematics and Physics, University of Ljubljana, Jadranska cesta 19, 1000 Ljubljana, Slovenia
[29] Institute of Plasma Physics and Laser Microfusion, Hery Street 23, Warsaw, 01-497, Poland
[30] Karlsruhe Institute of Technology, Hermann-von-Helmholtz Platz 1, 76344 Eggenstein-Leopoldshafen, Germany
[31] Laboratorio Nacional de Fusion, CIEMAT, Madrid, Spain
[32] Ecole Polytechnique Fédérale de Lausanne (EPFL), Swiss Plasma Center (SPC), 1015 Lausanne, Switzerland
[33] Department of Industrial Engineering, University of Rome 'Tor Vergata', via del Politecnico 1, 00133 Roma, Italy
[34] School of Science, Aalto University, PO Box 14100, Espoo, FI-00076 AALTO, Finland

E-mail: Xavier.litaudon@cea.fr

Received 27 November 2023, revised 27 February 2024
Accepted for publication 15 March 2024
Published 15 August 2024

Abstract

ITER is of key importance in the European fusion roadmap as it aims to prove the scientific and technological feasibility of fusion as a future energy source. The EUROfusion consortium of labs within Europe is contributing to the preparation of ITER scientific exploitation and operation and aspires to exploit ITER outcomes in view of DEMO. The paper provides an overview of the major progress obtained recently, carried out in the frame of the new (initiated in 2021) EUROfusion work-package called '**Pr**eparation of **I**TER **O**peration' (PrIO). The overview paper is directly supported by the eleven EUROfusion PrIO contributions given at the 29th Fusion Energy Conference (16–21 October 2023) London, UK [www.iaea.org/events/fec2023]. The paper covers the following topics: (i) development and validation of tools in support to ITER operation (plasma breakdown/burn-through with evolving plasma volume, new infra-red synthetic diagnostic for off-line analysis and wall monitoring using Artificial Intelligence techniques, synthetic diagnostics development, development and exploitation of multi-machine databases); (ii) R&D for the radio-frequency ITER neutral beam sources leading to long duration of negative deuterium/hydrogen ions current extraction at ELISE and participation in the neutral beam test facility with progress on the ITER source SPIDER, and, the commissioning of the 1 MV high voltage accelerator (MITICA) with lessons learned for ITER; (iii) validation of neutronic tools for ITER nuclear operation following the second JET deuterium–tritium experimental campaigns carried out in 2021 and in 2023 (neutron streaming and shutdown dose rate calculation, water activation and activated corrosion products with advanced fluid dynamic simulation; irradiation of several materials under 14.1 MeV neutron flux etc).

Keywords: nuclear fusion, tokamak operation, neutral beam heating and current drive, neutronics

Some figures may appear in colour only in the online journal

1. Introduction

ITER [1] is of key importance in the European research roadmap for the realisation of fusion energy [2, 3], as it aims to prove the scientific and technological feasibility of fusion as a future energy source. The EUROfusion consortium is contributing to the preparation of ITER scientific exploitation and is leveraging the ITER outcomes and lesson learnt in view of the EU DEMO design. The European fusion roadmap states '*To ensure its (ITER) success, a team is needed with deep understanding of the critical plasma issues and equipped with comprehensive validated modeling tools to design and optimize the plasma and its control*' [2].

In this context, a specific EUROfusion work-package has been created recently (the activity was initiated in 2021) called '**Pr**eparation of **I**TER **O**peration' (PrIO) to implement some elements of the preparation of EUROfusion's role in ITER operation and scientific exploitation. With a growing participation of EUROfusion members in the preparation of the ITER scientific programme, it is necessary to increase the integration and coordination of the relevant EUROfusion activities to provide coordinated EUROfusion inputs to the ITER organization (IO) and to position the EU laboratories to obtain maximum benefits from ITER operation. The term 'operation' should be understood in the global sense encompassing integrated commissioning, plasma operations, machine or subsystem operations etc, including the scientific and technical exploitation that need to be carried out well in advance of the formal start of the ITER operation. Indeed, in this paper, we cover more extensively the research, development and validation on existing EU facilities of the scientific and operational tools [4] to be compliant with ITER requirements and fully ready for preparing ITER operation.

This paper provides an overview of the activities performed within the EUROfusion work-package PrIO and gives a summary of the major progress and key achievements with lessons learned for ITER. It is supported by extensive contributions [5–18] presented at the 29th Fusion Energy Conference (16–21 October 2023), London, UK [www.iaea.org/events/fec2023]. The paper covers the following aspects:

(1) development and validation of tools on existing facilities to be transferred in support to ITER operation [7–12]: newly validate plasma breakdown/burn-through with evolving plasma volume, new infra-red synthetic diagnostic for off-line analysis and wall monitoring using artificial intelligence techniques, synthetic diagnostics development, multi-machine EUROfusion databases for model development and validation;
(2) research and development on the radio-frequency (RF) ITER neutral beam sources with different sizes in a step-ladder approach leading to long-pulse discharges in hydrogen (1000 s) and in deuterium at ELISE with controlled co-extracted electrons and participation in the first integrated ITER technology facility in operation, i.e. the neutral beam test facility (NBTF), with progress on the full size ITER RF source, SPIDER, with caesium (Cs) management, and, the commissioning of the 1 MV high voltage accelerator (MITICA) with lessons learnt for ITER [13–15];
(3) development and validation of nuclear codes, neutronic tools and experimental techniques for ITER non-nuclear and nuclear operation by taking advantage of the exploitation of the recent JET experimental campaign carried out in 2021 (and more recently in 2023) with a mixture of deuterium–tritium (called DTE2 in 2021 and DTE3 in 2023) leading to the significant production of 14.1 MeV neutrons [5, 6, 16–19]: neutron streaming and shutdown dose rate calculation, water activation and activated corrosion product with advanced fluid dynamic simulation; irradiation of a several materials under 14.1 MeV neutron flux. An outstanding amount of nuclear fusion relevant data has been collected in the frame of EUROfusion technological exploitation of JET deuterium–tritium operations, which was initiated in the Horizon 2020 Work Programme (called JET3 project) [20, 21], and it is currently ongoing within PrIO under Horizon Europe.

After this introduction and before the conclusion, the paper is structured along three main sections:

- Section 2 on the 'development and validation of operational tools for ITER';
- Section 3 on the 'development of RF sources for neutral beam injectors (NBIs) and contribution to ITER NBTF';
- Section 4 on the 'development and validation of nuclear codes for ITER'

2. Development and validation of operational tools for ITER

2.1. Plasma breakdown/burn-through simulation tools

ITER nuclear operation will require a plasma initiation scenario that is reliable, reproducible and at low-risk. A solid understanding of all aspects of plasma initiation and reliable/validated predictive modeling tools are needed in order to prepare ITER operation and to be able to make efficient and effective adjustments. A new electromagnetic plasma burn-through model has been developed (DYON) and statistically validated against ohmic plasma initiation data in MAST [22] and VEST (Seoul National University) [8]. Using operation signals available in a control room, the new tool enables consistent calculation of the time-evolving loop voltage with 2D time-evolving poloidal magnetic flux including plasma volume evolution during the plasma breakdown and burn-through phase (previously assumed fixed). Dynamic volume evolution is crucial for ITER prediction where large volume is reached after burn-through. The validity of the upgraded model has been statistically checked with 34 ohmic start-up discharges, which were randomly selected in MAST database. The experimental input data such as circuit current time traces,

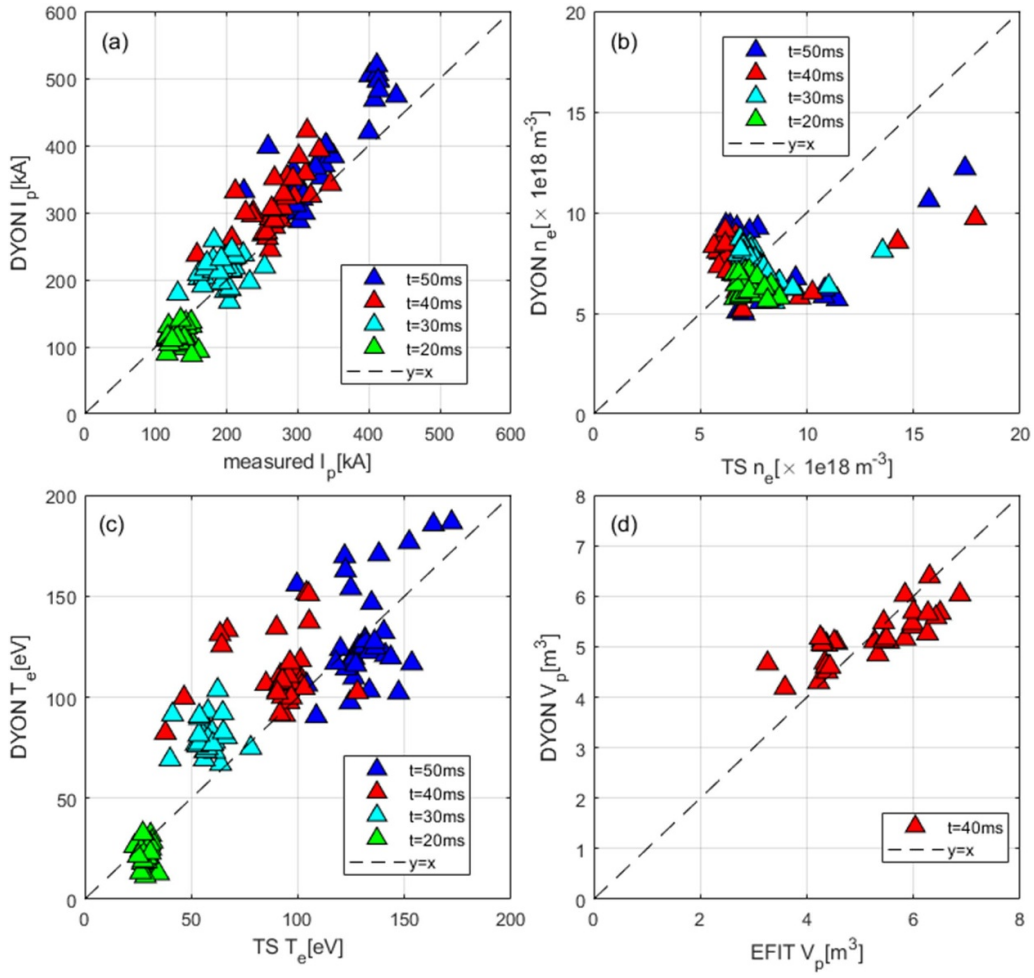

Figure 1. Statistical comparison between DYON plasma burn-through modeling calculation and MAST measurements: (*a*) plasma current, (*b*) electron density, (*c*) electron temperature and (*d*) plasma volume. Reproduced from [22]. The Author(s). CC BY 4.0.

prefill gas pressure, and gas puffing data were given for each discharge. The plasma currents (a), electron density (b), electron temperature (c) and plasma volume (d) were predicted by the DYON code and a good agreement with the measured data were found when using identical DYON setting as the one tuned for the MAST discharge #27512 as illustrated in figure 1.

The so-called CREATE-BD/BKD0/GRAY code is based on a tight coupling scheme between kinetic (BKD0), electron cyclotron (EC) wave absorption (GRAY) and magnetic models (CREATE-BD). EC heating absorption in ITER start-up has been assessed by systematically scanning various ITER parameters (neutral pressure, EC power, O vs X mode, impurities) [7, 23–28]. The breakdown operational domain and burn-through in devices with superconducting poloidal coil are limited by the maximum toroidal electric field (which is about 0.3 V m^{-1} for ITER) and can be expanded with the application of EC heating. The recent improvement to the CREATE-BD/BKD0/GRAY strong coupling optimization procedure as illustrated in figure 2 (left), consists in the automatic data exchange between CREATE-DB and BKD0 in the optimization of the control voltage waveforms to achieve breakdown and early ramp-up conditions. The simulation and optimization of the magnetic scenario for the entire start-up phase, including the early plasma current ramp-up has been successfully applied during TCV experiments [28]. The 2019 ITER breakdown studies have been extended to different possible ITER breakdown scenarios at 2.65 T and 5.3 T while injecting the EC beam either from the equatorial or from the upper launchers. In the studies, the central solenoid-poloidal field power supply voltages are limited to half of the full capability. The GRAY code implemented in Integrated Modeling And Analysis Suite (IMAS) has been upgraded to include multi-pass EC absorption via a simple reflection model at the first wall. The dependence of EC absorption on electron density and temperature has been assessed for the ITER first plasma start-up. The fraction of absorbed EC power as a function of electron density (n_e) and temperature (T_e) is reported in figure 2 (right) for both O-mode and X-mode (XM) injection. As expected, at low density, absorption is dominated by XM component generated after reflection at the inner wall. This fact stresses the importance of maximizing the fraction of power coupled to XM in the assumed first-plasma scenario. With XM a successful start-up scenario is

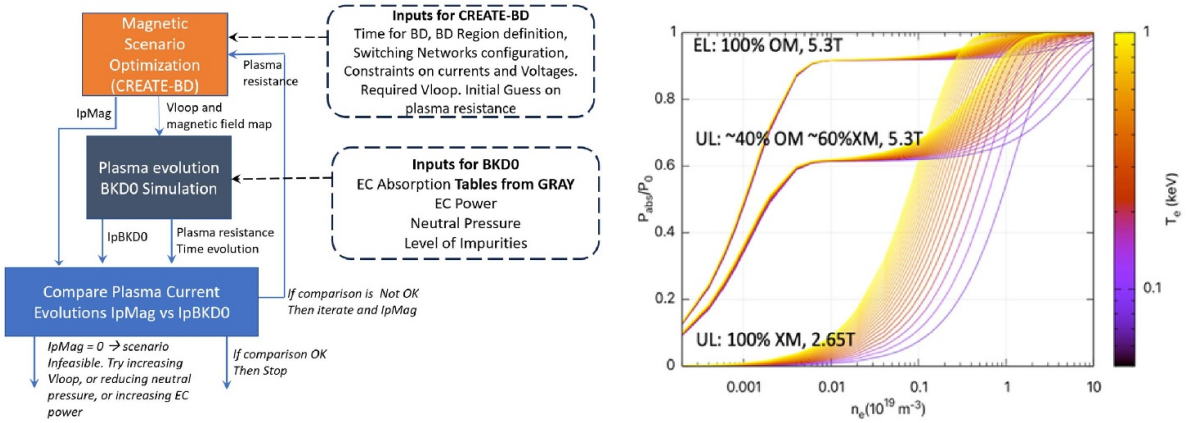

Figure 2. (left) General layout of the CREATE-BD/BKD0/GRAY coupling scheme for breakdown simulations; (right) ITER simulation: EC absorption for O-mode (OM) injection from EL and UL at 5.3 T and X-mode (XM) injection from UL at 5.3 T and X-mode (XM) injection from UL at 2.65 T. Reproduced from [7].

obtained with 1 MW of ECRH and a neutral pressure of 200 mPa.

2.2. *Infrared temperature synthetic diagnostic and thermal events detection algorithm*

Mastering high performance and burning plasmas in a nuclear environment is crucial for reliable, safe operation and machine protection. The infrared (IR) thermography system on ITER has been designed to monitor ∼70% of the first wall and divertor surfaces [9]. It should be capable, of measuring surface temperature with sufficient accuracy to detect anomalous behavior of plasma facing components (PFCs) between 200 to 3600 °C. Nevertheless, in metallic environments, IR measurement interpretation is challenging due to parasitic flux, variable and low wall emissivity. Infrared thermography temperature synthetic diagnostic has been developed and validated in present facilities for off-line analysis and real-time first wall protection [10, 29–31]. This novel approach contributes to improve IR interpretation in present facilities for reliable ITER application during plasma operation. For the development of the IR synthetic diagnostic, progress has been made along three tasks: (1) the development of an accurate and fast IR ray tracer code for the simulation of the camera image for any given plasma scenario [32]; (2) the experimental characterization and modeling of the materials optical properties (emissivity, reflectance) to establish a complete model of bidirectional reflectivity distribution function of in-vessel materials [33]; and, (3) the confrontation of IR synthetic diagnostic to tokamak experiences on ASDEX-Upgrade, W7-X and WEST in particular for discriminating thermal events to reflections features [29]. Figure 3 is an example of the experimental and simulated IR images for WEST where all parasitic reflections to the measured IR signal in tungsten wall have been identified with their precise origin (e.g. reflection from divertor or from antenna guard limiters etc) assuming a steady heat flux during the stationary phase.

In addition, the very first demonstration of simulated images during transient off-normal events, e.g. edge localized modes (ELMs), has been performed in 2022 [10] with a direct application to ITER geometry using data provided by the non-linear extended magnetohydrodynamic (MHD) code JOREK. An illustration of the integrated calculation is shown in figure 4 with the production of ITER IR synthetic images during one ELM cycle. JOREK is used to simulate the density distribution during transient events like ELMs (figure 4(*a*)). The JOREK volume data is then projected onto 3D surface of the PFC (figure 4(*b*)). Thermal analysis is performed to convert the power deposited on PFCs to the surface temperature using realistic boundary conditions (thermal properties of materials, cooling system) [34, 35]. As a first approximation, a 1D thermal model is used to calculate the temperature evolution during ELMs (figure 4(*c*)). As a next step, finite element methods should be used to include lateral diffusion of heat. The resulting 3D temperature field is then used as input of the ray tracing code, core of the synthetic diagnostics simulation tool, to propagate the rays within the 3D geometry taking into account the materials optical properties (i.e. emissivity and reflectance) (figure 4(*d*)). In the near future, similar type of calculations will also be performed to simulate IR images during disruption events.

The thermography diagnostic will be essential for ITER operation by providing (visible and IR) images and temperature measurements of the internal vessel components for machine protection (e.g. to avoid damages of internal components leading to a water leak in the tokamak vessel) and scientific analysis. The implementation of efficient real-time algorithms together with the large quantity of generated data to be processed during long-pulse operation call for the development of an automatic image processing system to detect and analyze all the thermal events. Artificial Intelligence with deep learning techniques based on algorithms trained on data set from existing facilities can provide an efficient way to detect, track and classify the thermal events with different physics origins [36–38]. Indeed, this repetitive and time-consuming

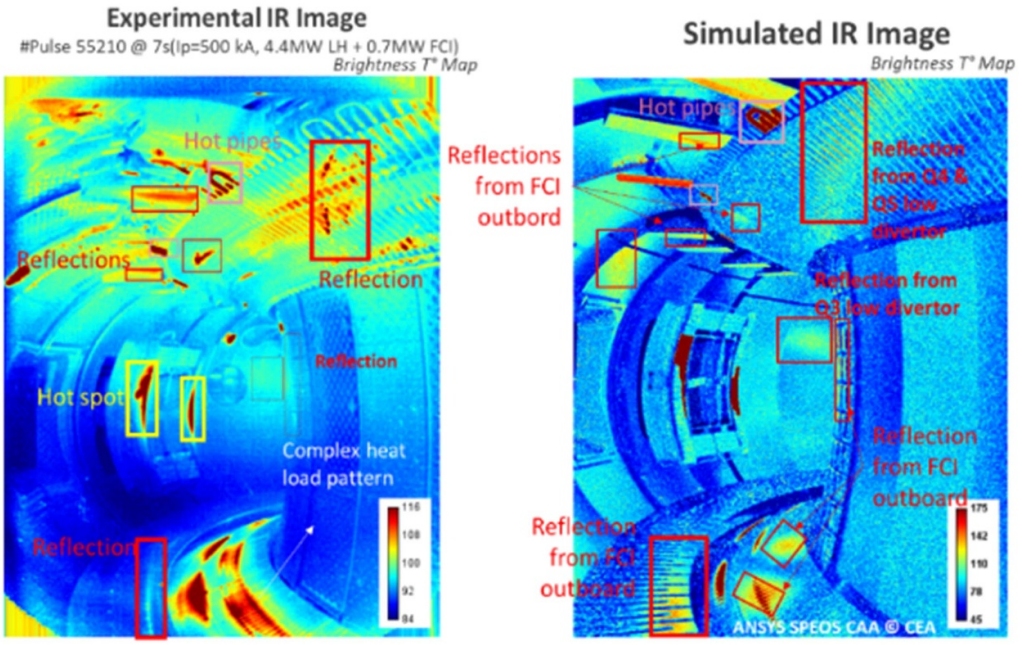

Figure 3. WEST experimental (left) and simulated (right) IR images calculated with the synthetic diagnostic. Adapted from [29]. CC BY 4.0.

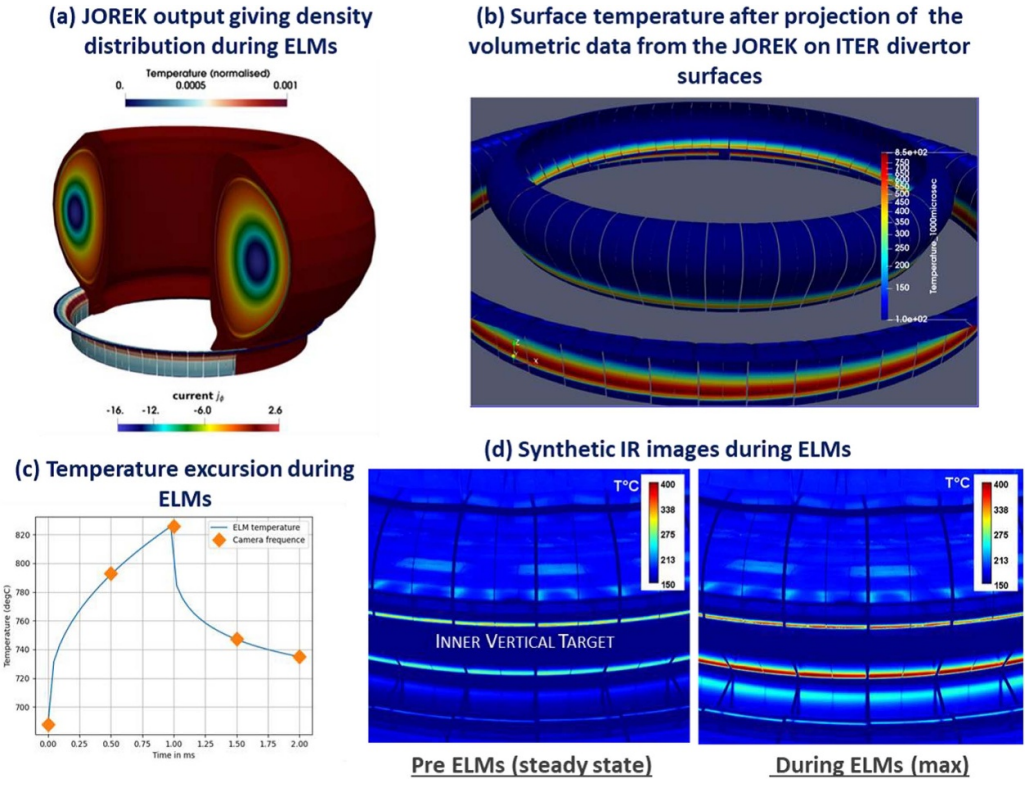

Figure 4. ITER simulation of transient ELMs in the IR synthetic diagnostic: (*a*) density distribution computed from JOREK, (*b*) volumetric data from the JOREK projected onto first-wall divertor surfaces, (*c*) temperature evolution, (*d*) synthetic images during ITER ELMs [10].

task is beyond the scope of the human analysis. For the automatic process, the quantification of the performance metrics (through a set of key performance indicator to be defined and tested) is essential to assess the capability of the model to achieve reliable automatic recognition of the thermal events (e.g. avoiding false alarms or missing off-normal events). In view of direct application to ITER operation, algorithm for automatic detection and classification of thermal events, based on artificial intelligence techniques, has been trained using a WEST IR image database where all the events have

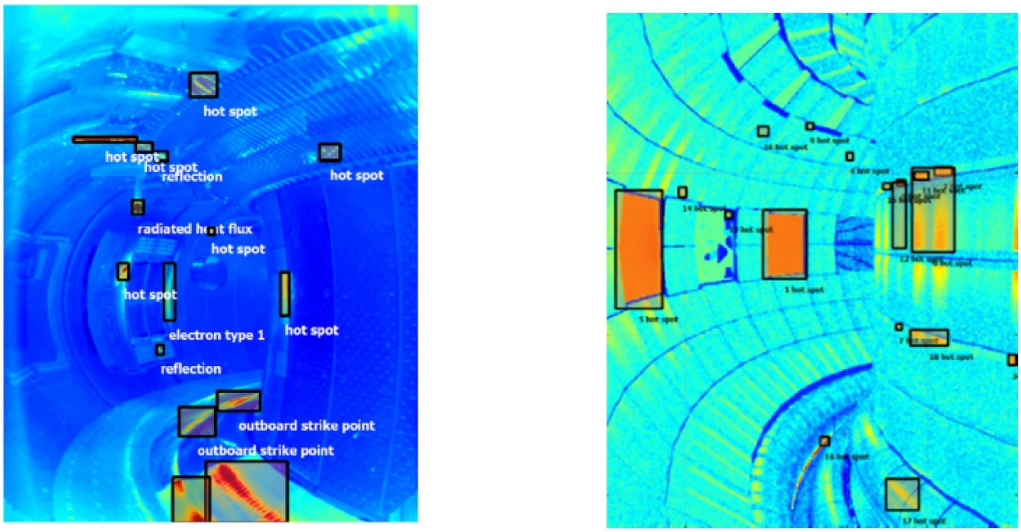

Figure 5. (left) WEST wide-angle IR images and automatic thermal events detection [Reprinted from [38], Copyright 2023, with permission from Elsevier]. (right) ITER simulated IR image where thermal events are automatically detected using algorithm trained on WEST data.

been manually identified based on the already acquired scientific knowledge [37, 38]. Then, the algorithm has been successfully applied for automatic detection and classification of thermal events for data (IR images) outside the selected database (figure 5 (left)). Finally, the hot spots and thermal events detection algorithm has been applied to ITER synthetic images produced by the synthetic diagnostic [10, 29–31] described in the previous paragraph. The initial results indicate that the algorithm trained on WEST data is able to automatically detect hot spots in ITER simulated images as illustrated on figure 5 (right). The ongoing development of a reliable performance metrics for a 'Zero-Day' automatic thermal events detection algorithm in view of ITER first scientific operation will be based on experience learnt on the existing facilities. Ultimately, real-time algorithms using automatic detection systems will be also developed and tested on real WEST experiments for direct application to ITER operation.

2.3. Fiber optics current sensor synthetic diagnostic

Standard magnetic sensors, arrays of different types of coils, are used in present-day installations to measure the plasma current and local magnetic field. However, in future long-pulse and burning plasma experiments, the performance of magnetic diagnostics could be compromised due to measurement drift caused by the combined effect of signal integration and the presence of nuclear radiation [39]. While novel magnetic probes and associated electronics based on Kalman observers were proposed to address this problem [39], it is sensible to consider additional risk mitigation strategies. Specifically, a non-inductive back-up solution for plasma current measurements has been proposed for ITER, relying on the Faraday effect induced by the magnetic field in the wave propagation in optical fibers. The system will provide back-up ITER plasma current measurements in steady-state regimes using a sensing fiber located on the outer surface of the vacuum vessel. This fiber will be subject to a harsh environment, which includes ionizing radiation, vibration, and strong magnetic fields, while measuring multi-mega-ampere range currents.

The EUROfusion activity has consisted of defining the algorithm for a FOCS synthetic diagnostics fully compatible with ITER requirements, which also incorporates the lessons learned from the FOCS experiments performed on Tore Supra [40] and JET [11, 41]. The influence of ionizing radiation, particularly the 14.1 MeV DT fusion neutrons, on the fiber polarization properties has been assessed during the JET DTE2 campaign. Two FOCS systems have been installed on JET and were used to perform current measurements during previous campaigns as reported [41]. More recently, during the JET D–T experiment performed in 2021 and for record discharges with a 14.1 MeV neutron fluence of the order of 1.6×10^{19} neutrons, good agreement between the FOCS and the reference Rogowski coil measurements is obtained within the measurement error bars of the two systems. Performing measurements in JET during the D–T campaign was a unique opportunity to address this aspect with a relevant D–T energy spectrum of neutrons.

The FOCS synthetic diagnostic has been developed to support JET analysis, provide a tool for optimizing the design of the real ITER FOCS diagnostic, and ultimately, support operation. Currently, it is anticipated that the ITER FOCS diagnostic will be installed in three different sectors distributed equally along the toroidal direction of the vacuum vessel. Each sector will host a single stainless steel tube containing one optical fiber. The tube serves as a boundary between the vacuum and non-vacuum regions, protecting the fibers from mechanical damage and allowing for fiber replacement. The EUROfusion activity involves the development of a Python computer code, compatible with IMAS requirements, to simulate the FOCS diagnostic at ITER. The FOCS synthetic diagnostic uses simulated tokamak environment data and information about the FOCS diagnostic system to compute a signal that replicates

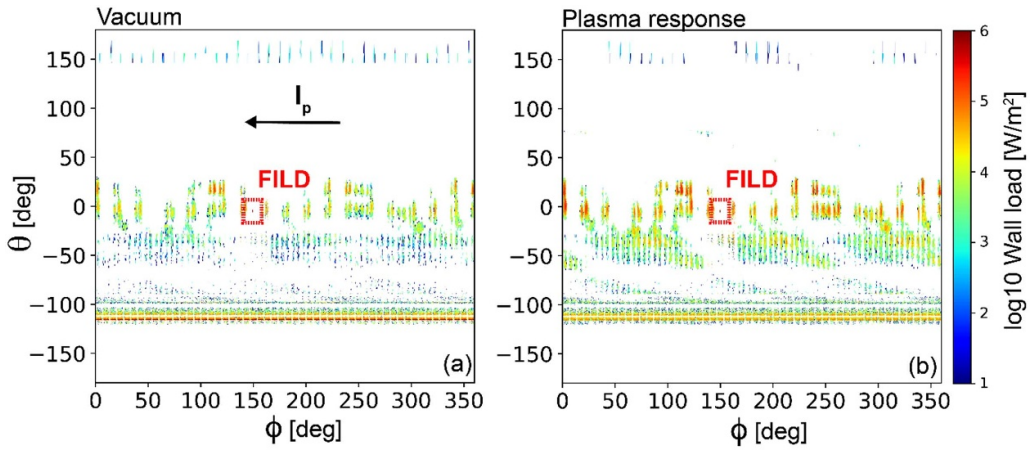

Figure 6. Simulated alpha-particle heat loads on the ITER first wall versus toroidal angle ϕ and poloidal angle θ in the presence of $n = 3$ magnetic perturbations for the baseline 15 MA scenario with two different assumptions: (*a*) the vacuum and (*b*) including the plasma response to the applied perturbation on the fast ion losses. The location of the FILD head is indicated with a brown box.

the output from the real diagnostic hardware. The propagation of input light with an initial wave polarization state is calculated in the fiber, following the real optical path, to generate a simulated optical signal (e.g. polarization state and signal power). Initial calculations with ITER parameters have been performed, incorporating different plasma current variations to validate the code.

2.4. ITER fast ion loss detector (FILD) diagnostic design and associated synthetic diagnostic

ITER is designed with the primary goal of sustaining burning plasmas with a dominant fraction of self-heating arising from the fusion-born alpha particles, with the objective of reaching and maintaining a fusion power amplification factor of $Q \geqslant 10$. Effectively confining alpha particles and understanding losses are crucial for the ITER project. Both fusion-born alpha particles and fast ions from auxiliary heating systems are susceptible to transport processes (neo-classical and anomalous), including those induced by a wide range of MHD instabilities. If fast ions are significantly redistributed or lost, it could substantially impact stability, confinement, and the efficiency of (self-) plasma heating and current drive, thereby jeopardizing the overall fusion performance of the machine. Under certain conditions, fast-ion losses become intense and highly localized, posing a risk to the integrity of the plasma facing components exposed to heat loads above the material limits [42].

In this context, ITER Organization has decided to implement a FILDs system [e.g. 43, 44] to measure the losses of alpha particles and fast ions generated by auxiliary heating systems during burning deuterium–tritium plasmas. The proposed diagnostic is based on an early conceptual design proposal [45]. It consists of a detector head equipped with a collimator, a scintillator plate, and an array of Faraday cups mounted on a reciprocating system. The scintillator's signal is transmitted through an optical transfer system, passing through the ITER Port Plug and Interspace. It then reaches a set of light acquisition systems, including cameras and photomultiplier tubes. EUROfusion has made significant contributions to implementing similar diagnostics in ASDEX-Upgrade [46, 47], TCV, and MAST-U [48] and is currently involved in the development of this diagnostic for JT-60SA [49]. EUROfusion has also recently contributed to the modeling activities carried out to estimate the fast-ion loss flux measured by the ITER FILD and its velocity-space structure. This activity will be carried out assuming a variety of plasma scenarios that take into account MHD instabilities and the imposed magnetic fields from coils to mitigate the ELMs on ITER. These tasks are essential for estimating the total signal measured by the diagnostic and for optimizing its design.

Recently, ASCOT [50] simulations have been used to estimate the fast-ion flux on the FILD head inserted into the ITER far scrape-off layer (SOL), considering resonant magnetic field perturbations (RMPs) with a principal toroidal mode number $n = 3$, which are externally applied by the set of ELM control coils. ASCOT simulations have been widely validated against FILD measurements in existing facilities [51–53]. The simulations include a realistic 3D wall, fusion born particles and the birth profile of the NBI sources. The simulations have been performed for the ITER baseline 15 MA H-mode quiescent plasma (i.e. without core MHD) where the detailed geometry of the FILD probe head is included in the 3D wall description to take into account the shape of the first wall panels as well as the 3D equilibrium with externally applied RMPs for ELM mitigation. The simulated fusion-born alpha particles heat loads distribution on the first wall, calculated locally along the poloidal and toroidal angles (respectively θ and ϕ), is illustrated in figure 6. It is found that the inclusion of the plasma response (including the plasma flow) on the particle losses reduces the total fast-ion heat loads on the wall from 4.2 MW to 1.9 MW. This reduction is visible in the divertor region on figure 6 (at poloidal angles around −120 Deg.). However, it is found that the power load on the FILD probe head is increased from 8.4 kW to 15.2 kW, as the plasma response shifts the

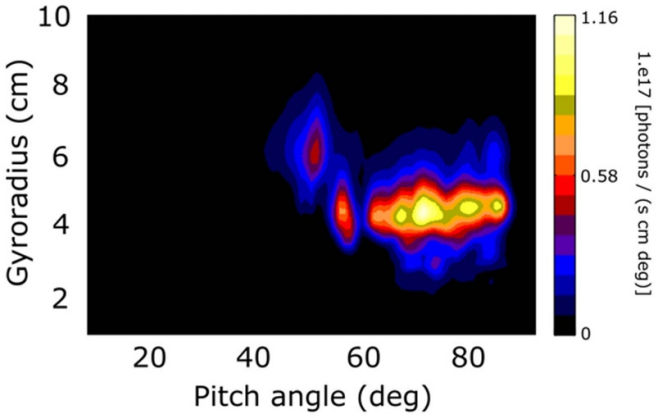

Figure 7. Simulated FILD measurements of the velocity-space distribution (as a function of gyroradius and pitch angle) of the escaping ions for ITER baseline scenario obtained with the synthetic diagnostic FILDSIM combined with an ASCOT simulation for calculating the fast ion losses at the diagnostic location.

perturbation pattern towards the FILD location. The future simulation work will consist to scan the FILD probe position to determine the optimal detector insertion depth in the scrappe-off layer (SOL).

The velocity-dependent flux of fast-ions that reach the vicinity of the FILD pinhole in the probe head is directly deduced from the ASCOT simulations. This information is then used to generate a velocity-space FILD synthetic/simulated images of the escaping fast-ion flux as illustrated by figure 7. The bridge between the ASCOT simulation inputs and the simulated FILD signal is provided by the synthetic diagnostic code called FILDSIM [54]. The code is an efficient tool for a direct comparison between experiments and simulations on existing facilities and for designing the ITER diagnostics based on past experience. The simulation of the instrument response is applied to these marker distributions by considering the probe head design from reference [45]. As a single collimator design is considered, only co-circulating particles at the FILD location are included. This geometry produced a collimator factor, as defined in [54], of 3%, meaning that 3% of the escaping particles arriving at the pinhole in the probe head will reach the scintillator detector. The simulated measurements of the velocity-space of escaping ions at the FILD location are depicted on figure 7 for the ITER baseline 15 MA scenario without core MHD. The simulated synthetic signal takes into account both the fusion-born alphas as well as the fast-ions injected by the off axis NBI source. The analysis of figure 7 indicates that the simulated signal around pitch angles of 60–80 degrees with a gyro-radius around 4 cm is dominated by beam ions losses, while the signal around a pitch angle of 50 degree with a gyro-radius around 6 cm has a dominant contribution from alpha-particles losses. These simulations also indicate that the emitted light from the escaping alphas and beam ions overcome the neutron background noise predicted by the neutronic Monte-Carlo (MCNP) simulations as initially discussed in references [44, 45].

2.5. EUROfusion multi-machine databases

For present machines and for ITER applications based on validated data, machine generic analysis tools have been developed and applied to populate multi-machine EUROfusion databases for addressing the physics of plasma core confinement, edge pressure pedestal in H-mode regimes [55–57] and disruption events [12, 58, 59]. The data are stored in a machine generic IMAS format including access methods and are compatible with the requirements of the International Tokamak Physics Activity (ITPA) databases. The EUROfusion coordinated effort consists in: (i) providing and maintaining up to date documentation of the database with common definition of the variables for the different machines, (ii) ensuring the systematic traceability of the data; (iii) ensuring that the experimental data are validated, and, regularly updated, and, (iv) releasing database description and version suitable for scientific exploitation and referencing in scientific publications. In this paper, an example is given for the multi-machine database on disruption which is one of the highest operational risk identified in the ITER research plan. For other applications of the EUROfusion databases not detailed in this paper, one can quote for instance, the exploitation of the pedestal database for developing/training new neural networks for estimating the pedestal parameters and upstream density using machine learning technics for fast and efficient self-consistent core-edge simulation in integrated modeling and extrapolation to ITER with derived uncertainty quantifications [56, 57]. The confinement database has been recently extended (up to 2665 pulses) with different hydrogen isotope mixtures (hydrogen, deuterium, tritium and deuterium-tritium mixture) with new data from JET and ASDEX Upgrade equipped with a metallic wall and the scientific exploitation is ongoing.

For the multi-machine database on disruption, the recent activities have focused on different aspects related to: (i) the continuous development and integration of the suite of tools for the validation of the disruption database, (ii) the population of a validated multi-machine database with data coming, so far, from JET, ASDEX Upgrade and TCV, (iii) the scientific exploitation supported by modeling activities [12, 58, 59]. The comprehensive and machine agnostic framework for the multi-machine database validation workflow called DEFUSE that stands for **D**isruption and **E**vent analysis framework for **FUS**ion **E**xperiments has been finalized (figure 8) with standardized definition of characteristic parameters and times of interest [12, 58]. Development is made to ensure reproducibility, data provenance tracking (data & code version control), and compatibility with the IMAS requirement. Disruption characteristic times and parameters are calculated through machine-agnostic modules, interfaced with the data of the various devices. The data are visualized and interactively validated through Graphical User Interfaces before being written in the database. Figure 9 shows an example of the fully automated calculation of characteristic disruption parameters for JET, ASDEX-Upgrade and TCV. Machine-dependent parameters, contained in data-dictionaries and template configuration files, are normalized according to the relevant machine

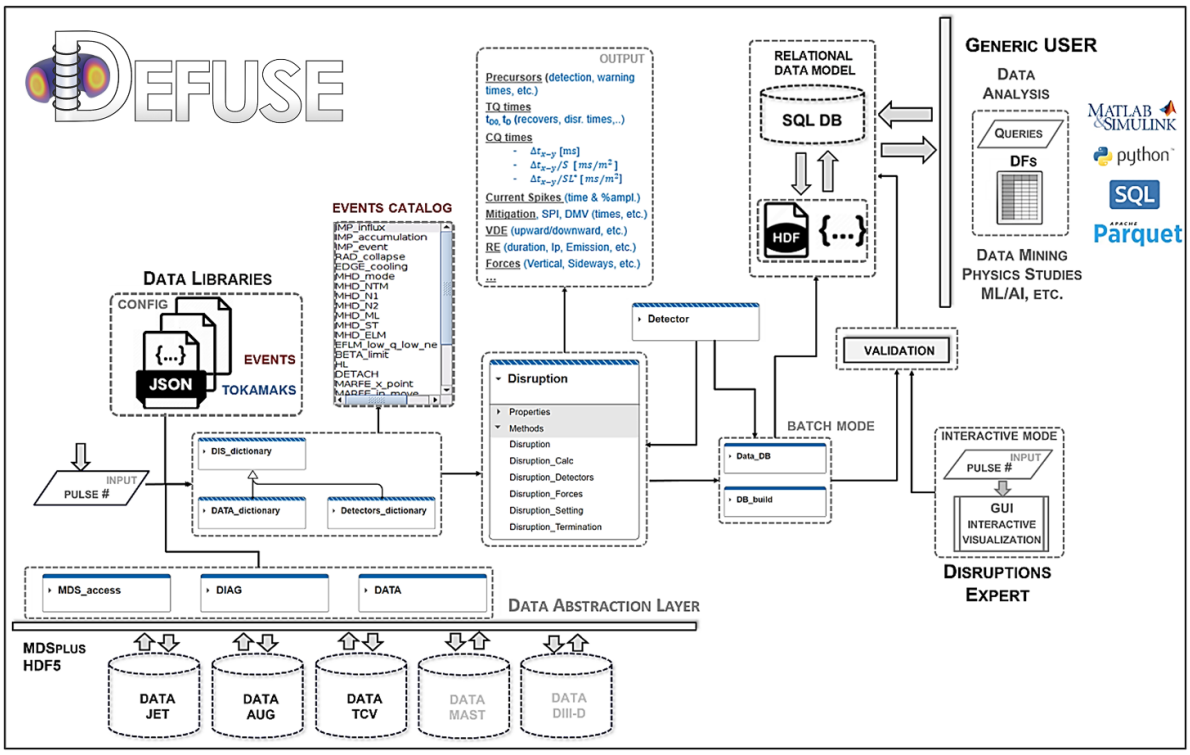

Figure 8. Schematic diagram of the disruption database Disruption database framework DEFUSE (**D**isruption and **E**vent analysis framework for **FUS**ion **E**xperiments). Reproduced from [12]. The Author(s). CC BY 4.0.

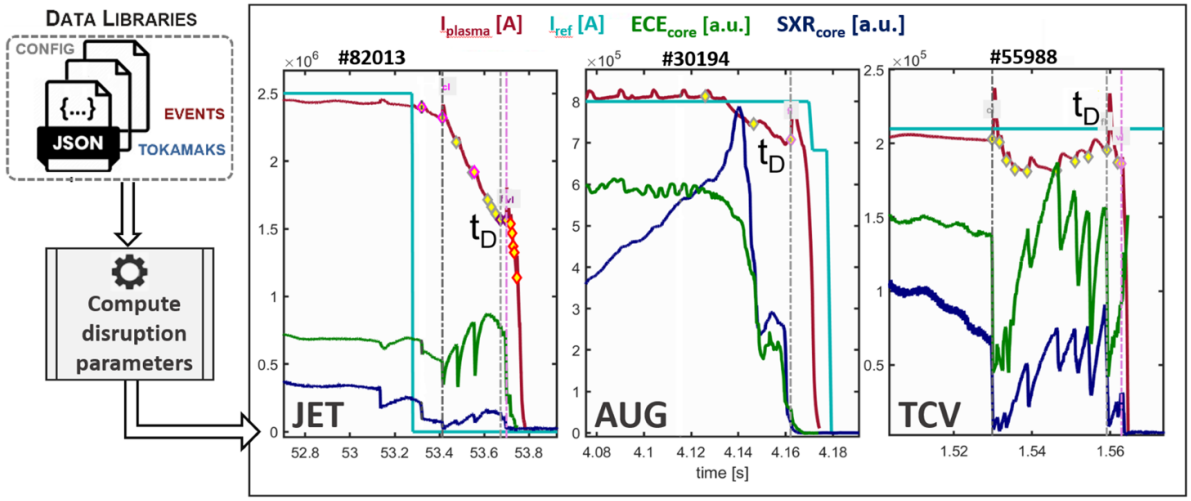

Figure 9. Automatic calculation of disruption characteristic times for JET, ASDEX-Upgrade (AUG) and TCV experiments based on the correlation of various quantities, where I_{plasma} is the plasma current, I_{ref} is the reference plasma current, $\mathrm{ECE}_{\mathrm{core}}$ and $\mathrm{SXR}_{\mathrm{core}}$ are proxies for the core temperature based respectively on electron cyclotron emission and on soft x-rays. Reproduced from [12]. The Author(s). CC BY 4.0.

timescales, and provide the basis for the calculation of standardized quantities. A key 2022 milestone is represented by the processing and data validation of the whole JET ITER Like Wall disruptions database (including induced disruptions with Massive Gas Injection) that includes more than 4000 entries from 2011 to 2022.

One application of the database is aiming at improving the physics understanding of the phenomenology characterizing density limits in tokamaks. These activities have led to the derivation of a first-principle scaling for the density limit [59]. A first-principles scaling law, based on turbulent transport considerations and the multi-machine database of density limit

discharges from the ASDEX-Upgrade, JET, and TCV tokamaks, shows a strong dependence on the heating power, therefore predicting for ITER a significantly larger safety margin than the Greenwald empirical scaling. A second application is the development of physics based disruption predictions methodology and tools that should be transferred to ITER first plasma operation. Initial application has been developed for the JET data with the ITER like wall using a statistical analysis to assess the distribution function of the disruption warning times for locked modes and radiative collapses. Indeed, both mechanisms can lead to the onset of tearing modes, which eventually lock and cause a disruption. This analysis has already provided key input for the optimization of JET real-time plasma termination schemes.

3. Development of RF sources for NBIs and contribution to the ITER NBTF

ITER will be equipped with two heating NBIs (with a provision of a third injector) and a neutral beam line for diagnostic purposes. An agreement was signed in 2019 between Consorzio RFX (Italy) and ITER Organization (IO) for the installation, optimization and operation of a test stand for full-size ITER negative ion source (SPIDER) for the heating and diagnostic systems, and a full-size ITER 1 MV NBI system (MITICA). These testbeds are part of the NBTF located in Padova, Italy, and aim to address two main technical challenges: the development of RF driven negative ion sources and the sustainment of high voltage [15, 60, 61]. The NBTF is realized with contributions (including in-kind components and plant systems) of the Consorzio RFX, European, Japanese [e.g. 62, 63] and Indian Domestic Agencies e.g. [64] with the support of IO and the EUROfusion collaboration of several European laboratories. The overarching objective of the NBTF is to contribute to the integrated optimization of the ITER NB system (16.5 MW per injector). The 1 MV high voltage system is designed to inject high-energy neutrals (870 keV hydrogen or 1 MeV deuterium) reliably into long-duration plasma experiments, lasting up to 1000 s in hydrogen and 3600 s in deuterium. The process involves RF driven negative ion source formation, acceleration, and neutralization, including the acceleration of a 40 A negative ion beam with controlled co-extracted electrons, i.e. acceleration to 1 MeV with low beam divergence ($<$7 mrad).

It was also agreed that the EUROfusion consortium will provide experts from European laboratories to work on the neutral beam project at ITER's NBTF facility with up to 14 professionals per year. Additionally, they will contribute to the development of reduced-size sources (1/8th size, BATMAN Upgrade, and half-size ITER-like RF negative ion sources, ELISE) [13, 14, 65–68] with up to six professionals per year. Europe has been actively involved in the development of RF driven ion source physics and technology [67] from the start, and, the ITER sources are based on a RF driven negative ion source that has evolved over several generations of prototypes at the Max Planck Institute for Plasma Physics (Garching, Germany).

Furthermore, the EUROfusion Operations Network was established in 2021 within the PrIO project [69]. This network initiated activities in 2022, and focused on specific aspects related to NBI operation in support of ITER with EU, Japan and IO experts' participation. Regular monthly 2 h seminars are held, covering dedicated NBI systems and related NBI research and development topics, such as protection systems, high-voltage conditioning, beam and transmission lines, diagnostics, and simulations.

3.1. Long pulse operation on BATMAN upgrade and ELISE

For RF driven negative ion sources development, the strength of the programme resides in a step-ladder approach with BATMAN Upgrade [68], ELISE [13, 14, 65–67], and, the full size SPIDER source before the integrated tests on MITICA at the NBTF [15, 60, 61] as illustrated on figure 10.

In its initial setup, the ELISE test facility was capable of performing short pulsed extraction only. While the ion source and its periphery, including the RF generators were capable of conducting CW pulses, short extraction blips embedded in long plasma pulses were possible only. These restrictions were primarily due to the constraints of the old High-Voltage power supply and the diagnostic calorimeter, which were not optimized for long-duration neutral beam pulses. To address the physics issues related to long-duration ITER-relevant neutral beam pulses, an upgrade of the ELISE test facility was initiated in 2021 and completed in the beginning of 2022. The upgrade focused on improving various aspects of the facility to enable long pulse operations and address key challenges, including beam optics, control of co-extracted electrons, beam uniformity and divergence, and Cs (caesium) management [13, 14]. The technical details of the upgrade are provided in reference [70] for the new high-voltage power supply and in reference [71] for the new diagnostic calorimeter. It is also worth mentioning that BATMAN Upgrade test facility is also ready for full steady state operation following the recent implementation of the last missing temperature controlled components (plasma grid and bias plate) and initial 1000 s experiment have also been demonstrated at BATMAN Upgrade in 2023. Investigations at BATMAN Upgrade are focused on long pulse operation with a MITICA-like extraction system and on beam optics studies for which the test facility has been equipped with several beam diagnostic tools [68]. These upgrades were essential to enhance the performance and flexibility of the facility for conducting long pulse neutral beam experiments.

For the Cs management in long pulse operation, it has been learned at ELISE that back-streaming positive ions created in the extraction system during beam extraction sputter Cs from the backplate which contributes to the Cs dynamics and counteracts the Cs depletion in long pulse discharges [72]. By upgrading the high-voltage power supply and the diagnostic calorimeter and gaining insights into the role of back-streaming positive ions in Cs management, the ELISE test facility has been enhanced to better simulate and address the challenges of long-duration neutral beam pulses, making it a valuable tool for testing and optimizing technologies relevant to the ITER neutral beam system.

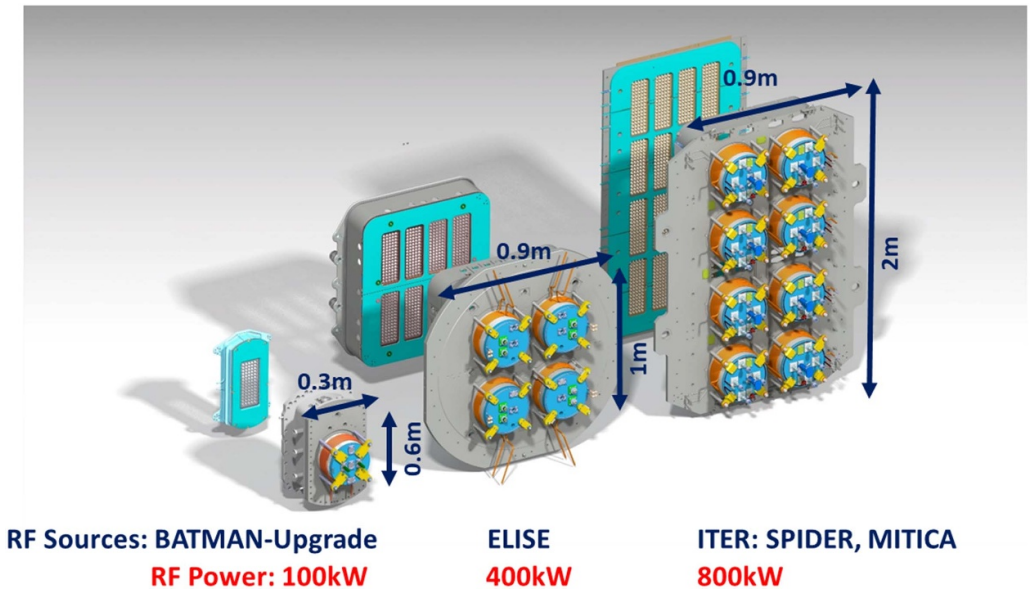

Figure 10. The RF sources development in a step-ladder approach towards ITER with the support of the EUROfusion facilities BATMAN Upgrade and ELISE. Adapted from [67], with permission from Springer Nature.

In 2021, the upgraded high-voltage system at the ELISE test facility was successfully tested with initial pulses in hydrogen, though at reduced parameters. Following the upgrade of the beam dump calorimeter, the system was used for experimental campaigns in both hydrogen and deuterium in 2022 [13]. During these experiments, it was demonstrated that stable operation is possible with pulses lasting up to 1000 s, which is the duration required for hydrogen NBI in ITER.

In hydrogen, stable operation allowed for the extraction of a very stable ion current of 19 A, with an electron-ion ratio well below one, as shown in figure 11 (left). In deuterium, an ion current of 12 A was extracted over 500 s, with the electron-ion density increasing during the pulse to a value slightly higher than one (figure 11 (right)). Time traces of the extracted ion current and the co-extracted electrons, measured separately for the top and bottom segments of the source, are shown in figure 11. During this initial 2022 experimental campaign, already 56% of the ITER targets for the heating system are achieved for the required 1000 s duration in hydrogen, along with about 42% in deuterium. These results represent the very first steady-state extraction at high performance for such long pulses [13]. However, in deuterium, a higher current of co-extracted electrons (2–4 times higher than in hydrogen) limits the source performance, as it reaches the technical limits for heat load on the extraction grids. To address this issue, a novel technique [13, 69] was used to bias the plate in front of the plasma grid, which helped stabilize and symmetrize the co-extracted electron currents. This technique is being considered for implementation in ITERs NBI ion sources.

The experiments at BATMAN Upgrade and ELISE are accompanied by a simulation program and diagnostics upgrades to gain further insights into the underlying physics and optimize the source performance. It is important to note that these pulses were conducted with a non-optimal caesium conditioning of ELISE, indicating potential for further improvements in future experiments. Overall, the results from the 2022 experimental campaign at ELISE demonstrate significant progress in achieving stable and high-performance steady-state extraction, providing valuable insights for the development and optimization of ion sources for the ITER NBI system.

3.2. SPIDER and MITICA at the NBTF

An integrated R&D activity is carried out in the dedicated NBTF to reach full NB performance in reliable condition. The facility consists of two main testbeds: SPIDER and MITICA. SPIDER is dedicated to the optimization of the RF driven negative ion sources at the scale required for ITER. It addresses various aspects of negative ion production and extraction, source uniformity, negative ion current density, and beam optics. MITICA focuses on a comprehensive integrated test of the full NBI system. Building on the experience and insights gained from SPIDER, MITICA conducts studies on beam acceleration, propagation, and beam optics. It also addresses critical aspects such as high-voltage holding in a vacuum, beam neutralization, and electrostatic removal of residual ions. By conducting experiments at the full-scale ITER level, MITICA aims to validate and optimize the entire NBI system, ensuring its reliable and efficient operation in the ITER environment. The involvement of EUROfusion experts in the NBTF is significant, as it allows for a collaborative and integrated approach to address the challenges and requirements of the NBI system. By working together as one team, experts from different European labs bring their specialized knowledge and skills to contribute to the success of the project. The operation of SPIDER since 2018 and its first caesium campaign in 2021 have shown promising results in achieving the required current densities and electron to ion current ratios for the ITER injector [15, 60, 61, 73–77]. As illustrated in

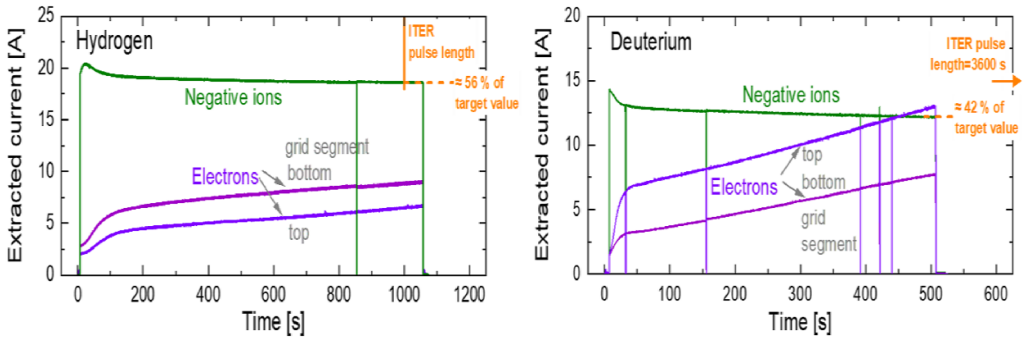

Figure 11. ELISE time traces of the extracted negative ion current and co-extracted electron current measured separately for the top and bottom segment of the extraction system during long pulses with the new CW high-voltage power supply in hydrogen (left) and deuterium (right). Reproduced from [13]. The Author(s). CC BY 4.0.

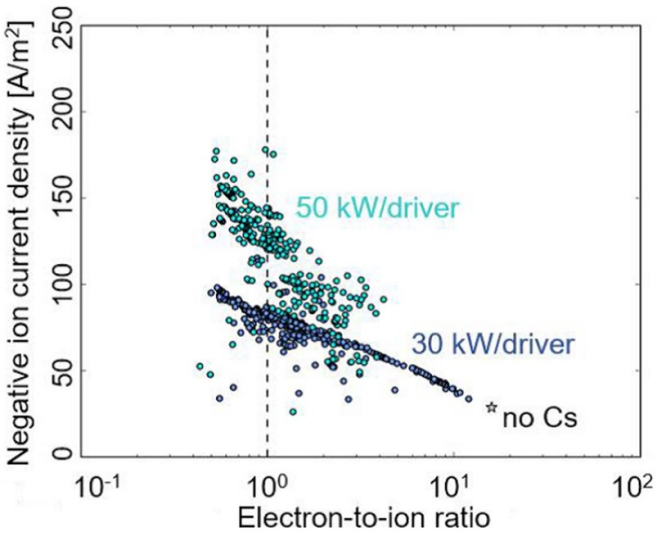

Figure 12. SPIDER accelerated current density versus the ratio of co-extracted electrons to ions current during the caesium campaign in hydrogen at 0.35 Pa [Adapted from [74]. © 2022 IAEA, Vienna. All rights reserved]. The entire history of the first caesiation campaign is shown performed in different operating conditions, starting from no caesium in the source (on the right-hand side). For this wide database analysis, the electrical current, as a proxy for the accelerated current density, is measured at a diagnostic calorimeter exposed to the beam. Comparing and interpreting the results of the various beam current meters available in SPIDER led to the conclusion that this is not an overestimate for the accelerated beam current, as discussed in references [78, 79]. ITER target of the heating & current drive NB is a ratio below one (dotted line) with a target accelerated current of 282 A m^{-2} in hydrogen plasmas in SPIDER with 85 kW/driver to mimic the expected ITER conditions with 7 grid accelerators. The entire history of the first caesiation campaign is shown, starting from no caesium in the source (on the right-hand side).

figure 12, the accelerated current densities obtained in hydrogen are in the range of 100 A m^{-2} to 150 A m^{-2} with RF power per driver of 30 kW and 50 kW of RF power per driver for an electron to ion current ratio close to or below unity [73, 74]. These initial performances are in line with the results of the previously described half-size RF ion source (ELISE) and scales to the ITER targets of the heating and current drive NB system (the extracted current density at the ITER RF source is 329 A m^{-2} in hydrogen and 286 A m^{-2} in deuterium whereas the accelerated current assuming 30% stripping losses in the accelerator is 230 A m^{-2} in hydrogen and 200 A m^{-2} in deuterium) when projected to a higher RF power of 85 kW/driver in hydrogen and up to 100 kW/driver in deuterium. The access to higher RF power values (up to 100 kW per driver) is presently limited by breakdowns formation in the RF circuits for which better pumping capacity is required to reach stable operation. The production of negative ions in the proximity of the plasma grid is accompanied by a reduction of the co-extracted electrons with caesium seeding and an increase of negative ion current (figure 12). The results have been obtained with a beam divergence of typically 12 mrad. These values, comparable to the measurement in the RF sources in ELISE and BATMAN Upgrade facilities, are higher than the ITER requirement of 7 mrad. Indeed, it was reported that the beam divergence was systematically higher in RF driven sources (>7 mrad) compared to arc-based sources (possibly due to the difference in negative ion temperature before the extraction) [76]. The favorable and observed beam divergence reduction with energy indicates that divergence below 7 mrad is achievable at 1 MeV [14, 15]. Since the divergence determines the beamline transmission and delivered power, it is crucial to understand the mechanisms and implications. In this context, further investigations concerning the divergence of a single beamlet and uniformity of a whole beamlet group are ongoing at BATMAN Upgrade supporting SPIDER investigations [13, 14]. In addition, a task force has been set by IO with ITER members participation to unify data analysis and methodology (on divergence and uniformity) for comparing results obtained from different facilities in EU and Japan with different diagnostics [14, 76, 77].

The optimization of ion current density, beam uniformity, and divergence remains a focus for further enhancements during the 2022–2023 SPIDER shutdown [61]. These enhancements include improvements to the RF driver to reduce cross-talk, cleaning and re-coating of plasma-facing components with molybdenum, and enhancements to the vacuum conditions with an enhanced pumping system to avoid breakdown in the RF circuits. In addition, the adoption of solid-state RF generators, to overcome the limits observed with the tetrode oscillators (e.g. frequency instabilities), is expected to improve

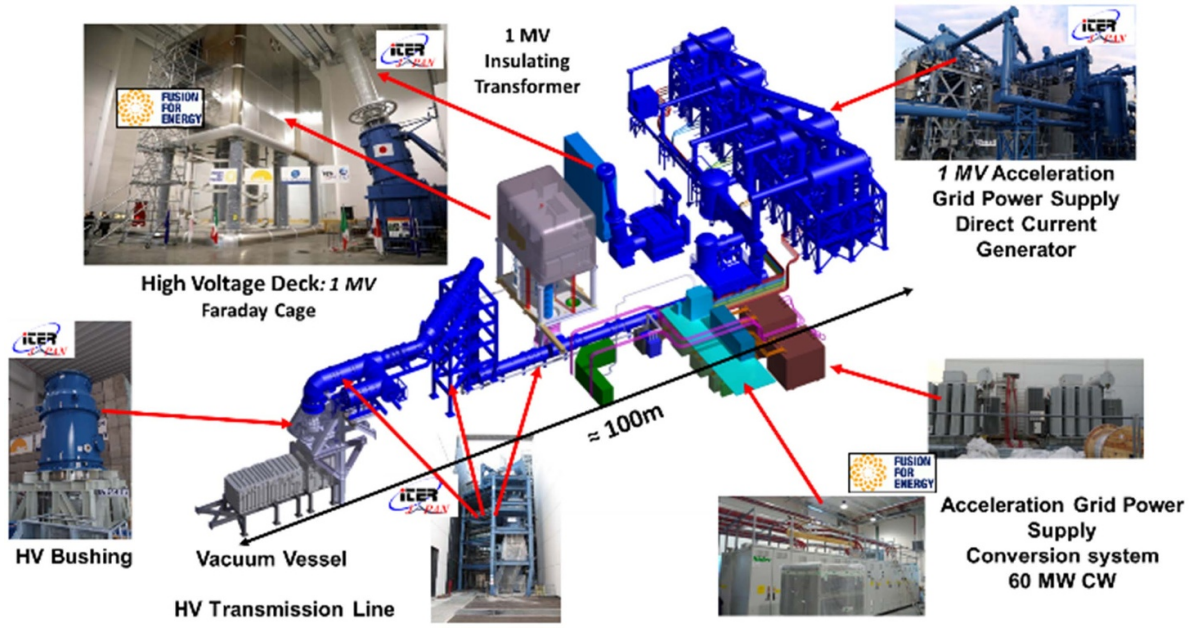

Figure 13. Overview of the MITICA power supply system [Adapted from [15]. The Author(s). CC BY 4.0]. The components in blue are provided by the Japanese domestic agency.

RF matching and coupling to the source at low filling pressure (0.3 Pa or below). Moreover, additional diagnostic capabilities and new confinement magnets at the beam source rear are being incorporated to further optimize the performance of the ion source.

In parallel to the SPIDER experiments, MITICA is under assembly while testing the first-of-a-kind high-voltage holding (1 MV) integrated electrical plant as illustrated in figure 13 [15]. During the integrated tests of 2021 performed together with the Japanese experts, power supply components have been damaged due to breakdowns events in non-identified positions of the high-voltage plant. Indeed, during no-load test operating the acceleration grid power supply and then, during high-voltage insulation voltage tests, two high-voltage breakdowns produced faults that damaged a 200 kV diode rectifier and the 1 MV insulating transformer. In this context, the recent 2022–2023 activities did focus on the:

(1) characterization and identification of the location of the high voltage breakdowns by installing specific measurements like visible cameras, Paschen discharge detection in air and gas, fiber optics;
(2) development of the electrical fast transients models validated by experiments at reduced voltage performed by provoking intentionally breakdowns in specific locations;
(3) simulations of the new protection systems in order to damp the large impulse voltages generated by the breakdowns that should be implemented for protecting the 1 MV insulation transformer and the 200 kV diode rectifiers in MITICA and in the ITER NB system.

A series of improvements to the insulation of some critical components have been introduced in combination with the use of new sensors sensitive to the presence of partial discharges, precursor signals of a breakdown both in air and in gas. Insulation tests carried out at the beginning of 2023 were successfully passed (1 MV DC applied for one hour followed by a series of ramps at full voltage) with reduced partial discharge activity. It follows that isolation has apparently been restored even if the tipping point has not been identified. Analyses of the collected data are still ongoing. Furthermore, a detection system derived from the one used during the tests will be definitively implemented both on MITICA and on ITER Heating NB system.

Detailed measurements and numerical analyses allowed to determine the dynamics of the events and to propose corrective solutions for implementation [15, 60, 61]. The development of ad-hoc fast transient models have allowed to explain the dynamics of the faults, highlight the weak points of the insulation with respect to breakdowns and to simulate additional protections. A conceptual protection system based on RLC type of circuit has been developed and the engineering design is presently ongoing. In the second half of 2024, the additional protections together with the new components to replace the damaged ones should be delivered on the NBTF site for installation to be completed by the end of 2024. The lessons learnt during the initial commissioning phase will be directly implemented in the final design of the ITER neutral beam system and have already highlighted the importance of having a NBTF in parallel of ITER construction and operation [15, 60, 61].

The voltage holding capability of the entire MITICA Beam Source at 1 MV is not fully addressed yet by experimental results and theoretical models available in the literature [80]. A specific HV test campaign is planned using mock-up electrodes in the MITICA Vacuum Vessel, reproducing in detail

the Beam Source and Accelerator geometry. If necessary, an intermediate 600 kV electrostatic shield will be placed between the source and the vessel. This campaign will be performed during the repair of the power supply and improvement and before installing the in-vessel components.

4. Development and validation of nuclear codes for ITER

4.1. Radiation environment during ITER non-nuclear phase

During ITER non-nuclear phase, fast ions, produced through a combination of NBI and RF heating, will interact with either plasma fuel ions or with the plasma impurities such oxygen or beryllium if the selected material for the ITER first wall remains beryllium. The interaction of the fast ions with the plasma impurities is expected to result in the emission of neutrons and gamma-rays. For example, plasma heating scenarios [81] relying on the Neutral Beam injection of 1 MeV energy range ions, or the acceleration of fast ion population by RF waves (ion cyclotron resonance waves), can trigger fusion reactions even in the non-nuclear operation phase (e.g. in hydrogen) with the beryllium as intrinsic metallic wall impurities (if beryllium is the a first wall material on ITER). To assess the effect of these fusion reaction on the radiation field and wall activation in ITER, a model for these neutron sources has been developed and validated against dedicated experiments performed at JET equipped with a beryllium wall and tungsten divertor. In addition, the relevant cross sections for the fast ions reactions with beryllium, i.e. ^{9}Be(p,$n\gamma$)^{9}B, ^{9}Be(^{3}He,$n\gamma$)^{11}C, ^{9}Be(p,d)2α, ^{9}Be(p,α)^{6}Li, ^{9}Be(d,$n\gamma$)^{10}B, ^{9}Be(α,$n\gamma$)^{12}C have been evaluated for the first time and will be submitted to the IAEA nuclear database [82]. Beryllium first walls exposed to intense gamma fluxes produce photo-neutrons via ^{9}Be(γ,n)^{8}Be (1.66 MeV energy threshold) that increase the dose, activate remote handling and transportation equipment. Whilst the photo-neutrons generated by prompt gammas during operations are negligible compared to the DT plasma neutron emission, at shutdown the decay gammas from neutron activation of materials will generate a delayed photo-neutron source that will increase the dose and activate remote handling and transportation equipment. For the first time, experimental evidence of this process has been revealed during the JET shutdown following the 2021 D–T experimental campaign indicating that nuclear operation with beryllium wall is challenging, and, requires validated tools for ITER radiation source estimations. It is worth noting that at the time of writing this publication, ITER organization [1] is proposing a new strategy to ensure the fastest path to the start of the nuclear phase, to minimize the technical risks, and, to minimize the licensing risks. Among others changes, it is proposed to replace beryllium with tungsten as first wall material. The consequences of the changes of wall material on the ITER radiation environment is beyond the scope of this publication and need careful assessment, including changes in neutron spectra, nuclear reactions in the non-nuclear phase, in material activation and production of radioactive wastes and dust. Finally, it should be stressed that the computational methodologies and modeling approaches developed and validated at JET with the beryllium-first wall can be extended to other plasma-facing materials, i.e. tungsten.

4.2. Neutron streaming and shutdown dose rates experiments and simulation

The second D–T Experiment (DTE2), carried out during the period August–December 2021 at JET equipped with a beryllium first wall and tungsten divertor, did produce a total yield of 8.5×10^{20} neutrons, which is nearly three times higher than the previous D–T experiment (DTE1) with a carbon wall (DTE1 in 1997 at a level of 3×10^{20} neutrons). This provides a unique opportunity to validate computational tools for the ITER assessment of shutdown dose rates (SDDR) due to neutron activation and neutron streaming under high 14.1 MeV neutron flux, reaching 10^{13} n cm^{-2} s^{-1} at the JET first wall. The methodology for the validation of tools is the one followed and refined across the previous JET D–D campaigns [17, 83–92].

Dedicated measurements have been performed with active and passive systems during JET operations and subsequent off-operational periods and shutdown (to measure the dose rate due to neutron activation). Twenty-two thermo-luminescent dosimeters (TLDs) and six activation foils (AF) have been located in several positions inside the torus hall and JET basement labyrinths to measure the neutron fluence. Additionally, three spherical ionization chambers (IC) have been installed at two ex-vessel positions: two ICs on a lateral horizontal port of JET octant 1 and one on the top of ITER like-Antenna port in octant 2 to measure the SDDR between plasma pulses and during shutdown. Figure 14 (left) shows the neutron yield for each plasma shot during the last two months of DTE2 (in the upper graph) and below, with the same time axis, the air kerma rate in μGy h^{-1} (i.e. the kinetic energy released in air per unit of time by charged particles created by the photon radiation) measured by the three ICs in octants 1 and 2. The benchmark of the computational tools for SDDR assessment in ITER is done in terms of air kerma rate, which is equivalent to absorbed dose rate in air as long as the condition of charged particle equilibrium holds. On the right side of figure 14, the neutron flux map in octant 1 as calculated with MCNP code during the highest D–T performance during DTE2 (JET pulse 99 971) is depicted (the iso-flux contour line at 10^{13} n cm^{-2} s close to the first wall is indicated). The neutron fluence level measured with TLDs and AFs was in the range of 10^{5}–10^{13} n cm^{-2}. It is worth mentioning that the level of neutron flux at the JET first wall is of the same order of the expected level in rear ITER blanket/diagnostic first wall for $Q = 10/500$ MW operation [83, 92]

The gamma radiation field due to neutron activation after DTE2 at JET is as intense as expected in relevant maintenance locations of ITER. In octant 1, close to the horizontal port, the SDDR measured by ICs is in the range $\sim$100 μSv h^{-1} to 10 mSv h^{-1}, while it is between $\sim$4 μSv h^{-1} and $\sim$1 mSv h^{-1} at the top of the ITER-like antenna (located in octant 2) at the end of the JET DTE2 campaign in December 2021. Such levels are relevant of expected conditions as in the ITER port

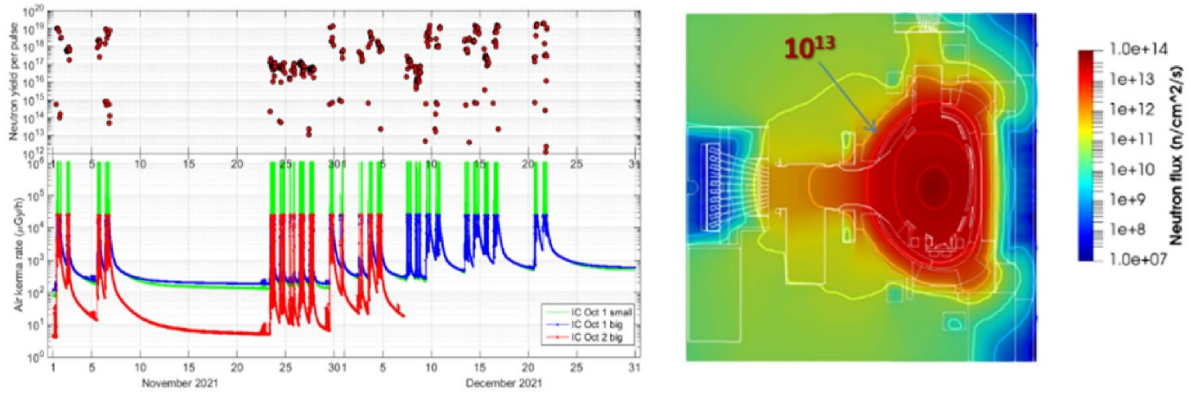

Figure 14. (left) measured neutron yield for each plasma shot (upper plot) and air kerma rate (in micro-gray per hour) versus calendar date during the last two months of DTE2; (right) neutron flux map in octant 1 for the JET D–T pulse 99 971 calculated by MCNP radiation transport code; contour line at 10^{13} n cm^{-2} s^{-1} has been highlighted.

interspace, where it is required a SDDR below 100 μSv h^{-1} after 10^6 s after plasma operation during the shutdown phase, and, for the port cell where it is required a SDDR below 10 μSv h^{-1} one day after the start of plasma shutdown. Accurate measurements are important for quantitative comparison to simulations, and, to reach this objective a careful analysis of influence quantities affecting measurements and of the experimental uncertainties was carried out.

The simulation of the neutron streaming experiments are performed using Monte Carlo N-Particle, MCNP, and TRIPOLI-4© codes for radiation transport and ADVANTG for improving the effectiveness of MCNP simulations. Various direct one-step and rigorous two-step SDDR tools are employed (i.e. Advanced D1S, R2Smesh, MCR2S, R2SUNED, D1SUNED, R2S, ORCS). These are based on a radiation transport code (i.e. MCNP) and an inventory code for calculating the neutron activation (e.g. FISPACT, ACAB, ORIGEN) and their validation for application to ITER is of paramount importance. Post-analysis and benchmark analyses are currently underway, deploying a set of state-of-the-art neutronics and SDDR tools. It is scheduled to complement these results during a third D–T experiment (DTE3) that recently took place in the autumn 2023 at JET. For new neutron streaming and SDDR data acquisition, new TLD measurements and AFs have been installed in the same positions as in DTE2. The validated determination of SDDR is an important contribution to estimate accurately the occupational radiation exposure (ORE) in future fusion nuclear facilities.

4.3. Test of neutron/tritium detectors for tritium breeder blanket

The online measurements of neutron and gamma fluxes and tritium production rate (TPR) in the harsh environments of fusion experiments, as expected for the ITER test blanket modules (TBMs) (i.e. temperature >400 °C, intense magnetic field and high level of radiation fluxes), require the proper development and testing of dedicated nuclear instrumentation. To address this need, a mock-up of the helium cooled pebble bed test blanket module was previously realized and tested at the Frascati neutron generator [93] before being installed at JET to exploit the intense neutron emission obtained during DTE2 for testing the detectors and validating the numerical codes used to predict breeding blanket performance such as tritium production [94, 95]. During DTE2, a single crystal diamond detector was successfully tested to simultaneously detect neutrons and measure the tritium production [95]. The tritium production measured by the diamond detector inside the JET TBM mock-up was found to be about 1.40 $\times$ 10^{-12} tritons per neutron. In addition to the experimental measurements, an extensive modeling programme has been initiated to simulate the neutron flux and the produced level of tritium using MCNP6 code. Three-dimensional simulations were carried-out using the integrated JET 360° model with FENDL3.1d nuclear data library under DT neutron emission from JET plasma. The ratio between the calculated and measured tritium production is in the range of 0.77–0.79, which is considered a promising result, indicating good agreement between the simulations and the experimental data and provides conservative estimation of the TPR. Finally, solutions for improving the measuring chain to obtain data at higher neutron rates (above 10^{15} neutrons per second) have been proposed and investigated in 2023 during the third D–T campaign (DTE3).

4.4. Activation and radiation damage of ITER materials

The experimental work at JET has focussed mainly on the evaluation of neutron activation and residual radiation fields of a range of ITER material samples, and at a lesser degree on the characterization of neutron induced damage in ITER functional materials [16, 96–98]. ITER functional materials for insulators or optical components as well as structural ones used in the manufacturing of in-vessel components have been exposed to neutron fluxes during JET D–D, T–T and D–T experimental campaigns using a long-term irradiation station (LTIS) with a material sample holder as shown in figure 15 (left) [96, 97]. The LTIS is located very close to the JET vacuum vessel just outside of the vacuum boundary. The materials considered include: Nb3Sn, stainless steel (SS316L) from a range of manufacturers, stainless

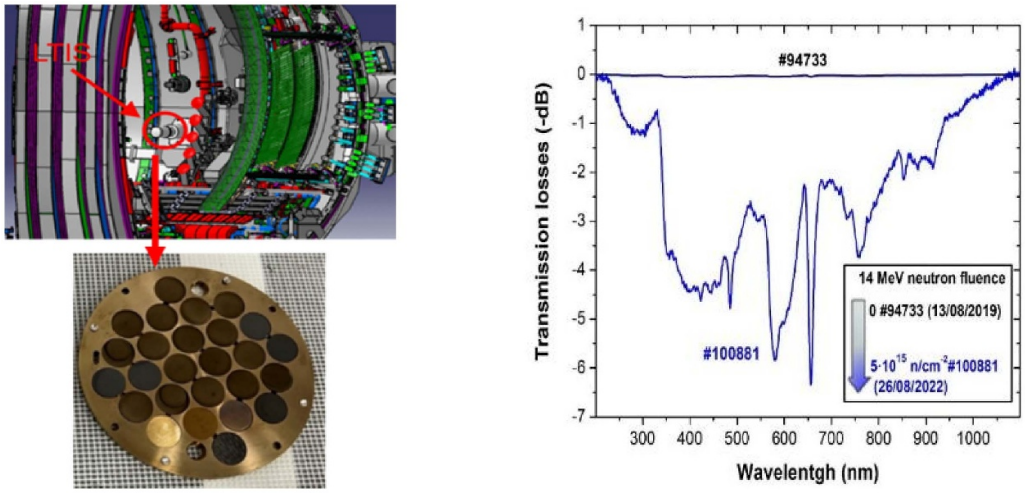

Figure 15. (Left) CAD drawing of the JET vessel section with the LTIS; picture of the LTIS sample holder taken after DTE2 with the irradiated ITER sample materials and dosimetry foils. (right) Transmission losses of silica optical fibers optics versus wavelength (nm) after neutron exposition during JET D–D, D–T and T–T experimental campaigns. The losses are normalized to the initial value before D–T neutron pulses (pulse #94733).

steel SS304B, Alloy 660, Be, W, CuCrZr, OF-Cu, XM-19, Al bronze, NbTi, EUROFER and silica optical fibers. The LTIS holder was installed into JET on 4 October 2020 prior to irradiation in the D–D, T–T and D–T (DTE2 carried in the second semester of 2021) experimental campaigns and was removed on the 25 September 2022. Then, the samples were distributed to different EU laboratories for analyses and gamma spectra measurements to identify and quantify nuclide activities generated through neutron activation. The measured contact dose rate of the LTIS following retrieval was 660 μSv h^{-1} comparable to the simulated value of 673 $\pm$ 75 μSv h^{-1} which validates the calculation methodology. The post-irradiation specific material radioactivity (in Bq/g) is calculated using FISPACT-II [99] and Monte Carlo N-Particle codes with a detailed JET model and materials specifications of the LTIS sample loading configuration. From D–D material activation analysis [16, 96, 97], the calculated post-irradiation materials specific activities (Bq/g) are close to the experimental data, with the exception of deviations in some samples that are attributed to impurity levels that may deviate from the material specification certificate. This effect and related uncertainty are important to be taken into account to assess activity levels of ITER materials at the end of the nuclear operation (decommissioning, waste process).

Optical and dielectric materials are important components in fusion reactors and the effect of nuclear radiation in real tokamak experiment with relevant 14.1 MeV fusion spectra needs to be assessed. Functional materials like hermetically sealed metal-coated pure silica optical fibers have been exposed at JET (using the LTIS) to neutron irradiation with a total cumulated fluence of around 5 $\times$ 10^{15} neutrons cm^{-2}. It is shown on figure 15 (right) that the optical transmission is reduced in the exposed fibers at wavelength ranging from UV to near IR. This mechanism has direct application for fusion facilities since silica and optical fibers are essential in diagnostics. It is important to monitor the performance of these optical fibers when exposed to radiation, as they may eventually need to be replaced.

In addition to optical fibers, other insulator materials subjected to radiation damage will be studied extensively following JET DTE3. Indeed, several materials (single-crystals, ceramics and amorphous phases such as Al_2O_3, SiO_2, $MgAl_2O_4$, YAG, Si_3N_4, AlN, CaF_2, and BaF_2) have been exposed during the third JET DT experimental campaign (2023) to 14.1 MeV neutron fluxes and will be removed for analysis (2024) in dedicated labs to further characterize their properties modification such as optical absorption, photoluminescence, reflectance, losses etc.

4.5. Neutron irradiation of electronic components at JET

The interaction of neutrons with components used in electronic circuits can lead to various detrimental effects, including damages or destruction of electronic devices, corruption of signals, errors in data or programs stored in electronic circuits (such as memories and microprocessors) [100–102]. These effects can occur gradually over time due to time-integrated cumulative phenomena or instantaneously from a single neutron interaction with the material, the latter known as single event effect (SEE). To assess the sensitivity of electronics to neutron-induced SEEs in the neutron environment of a fusion facility and to compare it with the sensitivity in the natural terrestrial atmospheric neutron environment for which electronics components are typically qualified by manufacturers, first of a kind experiments were conducted at the WEST (tungsten environment in steady-state tokamak) facility. In these experiments, a set of about 3 Gbit of statistic random access memory (SRAM) components, specifically 65 nm bulk

SRAMs fabricated by STMicroelectronics, were exposed to neutrons emitted from fusion reactions in deuterium thermonuclear tokamak plasmas [100]. To further investigate and validate the findings, additional laboratory tests were performed using mono-energetic neutron sources, such as those at the GENESIS and AMANDE facilities in France, to irradiate the same electronic components. The comprehensive set of experiments has highlighted the importance of high-energy neutrons generated during tritium burn-up, specifically the D–T reaction from the low level of tritium produced by the D–D fusion reactions, in explaining the recorded events during the WEST experiment [100]. These findings have led to the expansion of the experiments on the WEST facility by exposing the same electronic components to a neutron flux produced by a D–T plasma on JET during DTE3 that took place in September–October 2023. Additionally, other components for accelerators electronics, specifically 40 nm bulk SRAM produced by Integrated Silicon Solution Inc., were tested in collaboration with CERN [102]. To interpret the experimental results and validate the models used to quantitatively estimate the neutron-induced error rates in the electronic components in view of application to fusion devices, it is crucial to measure the local neutron flux and energy spectrum at the location of the components to be tested. For this purpose, a neutron spectrometer called DIAMON (Direction-aware Isotropic and Active MONitor) from Raylab has been installed close to the components. The test-bench (picture in figure 16), with neutron spectrometer and electronic circuits, has been installed on the 1–2 July 2023 in the basement of the JET torus hall (south-east corner) already equipped with TLD for the neutron fluence measurements (c.f. streaming experiment described in section 4.2), and is remotely controllable. This installation allowed validation tests to be performed before DTE3, fully exploiting the D–D plasmas. Results from D–D and D-T plasmas have already been obtained and preliminary results indicate (despite the expected different energy spectra) the suitability of equipment location for obtaining good measurement statistics with relevant neutron spectra ranging from thermal to fast neutrons with energy up to 14.1 MeV, while not destroying the electronics that control the test bench thanks to the existing shielding provided by the concrete slab between the JET torus hall and the basement. Once the models are validated on WEST and JET, they will be applied for a comprehensive study on the sensitivity of modern electronics to neutron-induced SEEs [101]. The results of this extended study will contribute to the qualification of the electronics in a fusion neutron environment.

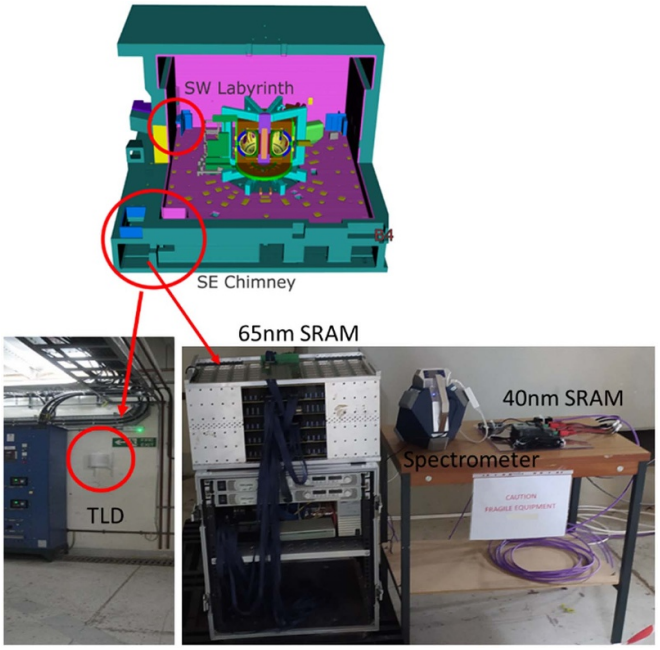

Figure 16. Picture of the test bench equipped with 65 nm and 40 nm SRAM components and the DIAMON neutron spectrometer as installed in July 2023 in the basement of the south east-corner of the JET torus hall (top view) already equipped with the TLD assembly of the streaming experiment.

4.6. Activation of cooling water

Activation of cooling water due to high-energy neutrons needs to be accurately predicted, as it represents a significant concern for radiological safety. The radioactive products of the reactions $^{16}O(n,p)^{16}N$ (threshold energy of 10.2 MeV) and $^{17}O(n,p)^{17}N$ (threshold energy of 8.5 MeV) are intense, albeit short-lived, decay gamma and neutron emitters which induce nuclear responses in tokamak and plant components [18, 103–112]. When the activated cooling water is pumped out of the vessel, the decay emissions from ^{16}N and ^{17}N induce nuclear responses in sensitive tokamak and plant components such as superconducting magnets, plastic polymer sealants, and electronics. Accurately quantifying this activation for fusion facilities is central to fulfilling radiological zoning requirements, ensuring the safety of the public and the maintenance workers, and compatibility with the operation of radiation-sensitive systems such as superconducting magnets, electronics (cf section 4.5), or plastic polymers [103].

The level of complexity of the water activation depends on various factors, including the velocity field and the irradiation scenario. To predict the activation of water flowing in arbitrarily complex 3D geometry, flow regimes and neutron fields requires full coupling of activation with fluid-dynamics physics models. No such tools were available until recently but, in recent years, EUROfusion and F4E have sponsored the advent of several of these [110–113]. A new open-source code called FLUNED has been recently developed [18, 106]. FLUNED calculates fluid activation by coupling computational fluid dynamics simulations with neutronics calculations. The code performs a completed computational-fluid-dynamics simulation of the water and evaluates the generation, propagation, and spontaneous decay of a radioactive species within the fluid. An open-source strategy has been adopted for FLUNED to facilitate its development, code verification and validation within the fusion community. This approach allows for easier

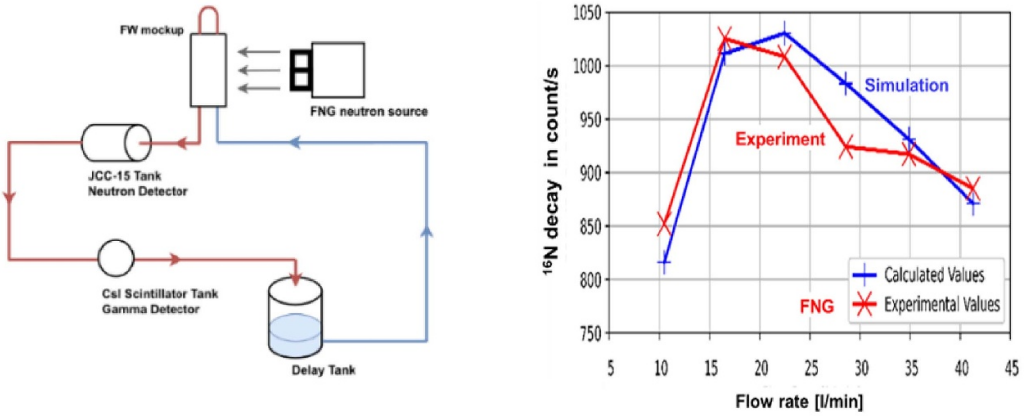

Figure 17. (left) Water activation experimental set-up at FNG with the neutron (Inventory Sample Neutron Coincidence Counter model JCC-15) and gamma CsI detectors and water expansion tank to increase the count rates [Adapted from [107], Crown Copyright © 2020, with permission from Elsevier]; (right) ^{16}N decay in FNG water activation experiment: experimental & simulated ^{16}N decay counts with FLUNED versus flow rate when the neutron source was positioned at a distance of 5 cm from the component [Adapted from [106]. CC BY 4.0].

collaboration, sharing of knowledge, and collective improvement of the code for training, research and development, and its application in ITER and DEMO projects.

The initial validation of FLUNED has been carried out using past measurements obtained from the December 2019 experiments performed at the Frascati Neutron Generator (FNG). These experiments, sponsored by F4E, involved irradiating an ITER actively cooled first wall mock-up component with 14.1 MeV neutrons [93, 107, 114]. The FNG neutron source was positioned at a distance of either 2 cm or 5 cm from the ITER first-wall components mock-up, and six water flow rates were selected, ranging between 10 to 42 l min^{-1}. The experimental water loop is depicted in figure 17 (left). To perform a precise comparison with the experimental data, the following quantities were computed: (i) the production rates of ^{16}N and ^{17}N in water; (ii) the generation, transport, and spontaneous decay of the nitrogen isotopes in the main components of the circuit; (iii) the count rates in the neutron and gamma ray detectors (as synthetic diagnostics). The direct comparison between the calculated and experimental count rates shows an excellent agreement between the two quantities as illustrated in figure 17 (right) for the gamma emissions. This successful comparison provides the first validation of FLUNED for studies of water activation.

To complement this first validation study, two new and dedicated experiments are planned and are being executed: (i) at JET during the last D–T campaign (DTE3) in 2023, and, (2) at the fission reactor TRIGA Mark II utilizing a closed-water activation loop (figure 18) [109].

The JET experiment will provide an integrated test in a real tokamak environment to be exploited for the validation of the codes and tools used for ITER assessment of water activation loads [83, 84]. After an initial feasibility study [108] and successful proof of concept tests following DTE2 in 2022, it has been recently decided to install in 2023 two gamma spectrometers, i.e. sodium iodide (NaI) and bismuth germinate ($Bi_4Ge_3O_{12}$) a.k.a. BGO scintillators, along with dosimeter (spherical IC), in the JET basement close to the cooling loop of the duct scraper of one of the NBIs (located on JET octant 4, as illustrated in figure 18 (left)). These detectors have provided online and local measurements of the energy spectrum and gamma dose rate during JET operation (with or without plasmas). Detailed Monte-Carlo particle transport and material activation calculations have been performed to prepare the experiment, optimize the detector position and shielding, and prepare for *in-situ* calibration of the gamma ray detectors. The experimental data will be used to validate multi-physics modeling methodologies in view of ITER application.

In parallel, a new closed water activation loop, called KATANA, is being constructed at the fission research reactor TRIGA Mark II at the Jožef Stefan Institute (JSI), Slovenia [109], as shown in figure 18 (right). The KATANA irradiation facility will serve as a well-defined and stable 6–7 MeV gamma-ray source, complementing JET and FNG experiments with new water activation experiments. These experiments will include shielding experiments using ITER-relevant materials, calibration of radiation detectors, investigation of short-lived moving radiation sources, and validation of computational codes and methods. The loop has been successfully commissioned in the second semester of 2023 for a series of experimental campaigns starting in 2024. Application and validation of FLUNED and other general-purpose activation-computational fluid dynamics tools in the planned water activation experiments at JET and the JSI-TRIGA reactor will enable the use of reliable simulation tools to study some ITER actively cooled components. This will allow for the reduction of expensive safety factors, as these tools can provide accurate predictions and assessments of water activation levels in these components.

4.7. Activated corrosion products experiments and simulation

In fluid circuits like water coolant loops, corrosion, erosion and dissolution of materials can lead to the mobilization of

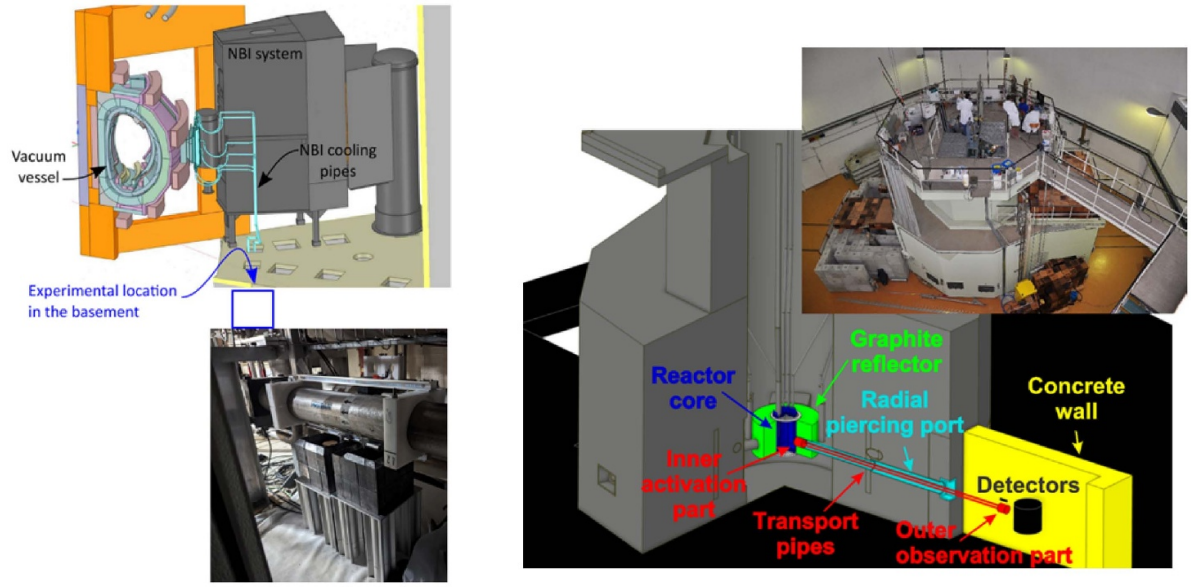

Figure 18. (left) JET water activation experiment: NBI duct scraper cooling loop equipped with shielded gamma ray detectors located in the basement under Octant 4; (right) KATANA, the new closed-water activation loop at JSI TRIGA Mark II research reactor. Adapted from [108], Copyright 2021, with permission from Elsevier. Adapted from [109], Copyright 2023, with permission from Elsevier.

metal dust particles and ions into the water loop circuit. In fusion (and fission) cooling systems, where these circuits pass through high neutron flux regions, the water and any corrosion products become activated. These activated materials, carried by the cooling water fluid, reach the ex-vessel regions of the tokamak that are accessible to workers during maintenance periods. Therefore, quantifying the activity of activated corrosion products (ACPs) is crucial for identifying the source of radiation exposure, optimizing ORE, managing radioactive waste, and defining maintenance plans for nuclear experiments like ITER and DEMO. However, little is currently known about the corrosion products and the rate of corrosion expected in fusion environments.

The reference code for ACP assessment within the fusion community for ITER is OSCAR-Fusion [115], which is a version of the OSCAR code developed by the CEA in collaboration with EDF and Framatome [116] specifically adapted for fusion conditions. However, this code has been mainly validated experimentally under fission reactor conditions, as very limited data exists for fusion-relevant conditions. Due to the different operating conditions in fusion (neutron spectra, materials, circuit geometry, chemistry and thermodynamic conditions of water including temperature, velocity etc), dedicated validation experiments need to be designed and conducted.

In this context, a comprehensive scientific methodology is being developed within EUROfusion for assessing the dose contribution due to ACPs in ITER-relevant conditions. The plan involves designing and carrying out new and dedicated experiments at the 14 MeV FNG. The objective is to validate the OSCAR-Fusion code and its approach used for estimating the radiation dose and dose rate due to ACP in fusion facilities.

To precisely quantify the ACP physics, a multi-physics approach is being developed that takes into account the operational scenario, thermo-fluid dynamic conditions, water chemistry, neutron irradiation, and material properties. To prepare for and guide the FNG experiments, a feasibility study was performed in 2022 by simulating the FNG water cooling loop in different experimental scenarios using OSCAR-Fusion. Given the constraints of the facility (limited time/neutron flux for continuous irradiation), the feasibility study has concluded that it is not possible to study corrosion products directly generated by the water flowing in the FNG loop. Instead, the proposed approach involves injecting an external source of calibrated and activated dusts and ions into the water circuit to mimic the ITER pipes' materials (such as copper or stainless steel, SS316L) activated under a 14.1 MeV neutrons source. This will allow studying the transport, deposition, and precipitation of ACPs. The initial experiments will be performed with test pipes made from copper, and the complexity level will be increased progressively, as already suggested and simulated. To mimic the complexity of the ITER pipe networks, the study will include some components as bends, manifolds, filters, variable diameter tubes. Additionally, to study the deposition of copper dust on stainless steel, a section of test pipe made from stainless steel will also be included. This comprehensive approach aims to provide crucial insights into ACP behavior and its impact on radiation safety in fusion devices.

4.8. Neutronics and virtual reality coupling for maintenance operation

A methodology is being developed to assess on one hand the potential of machine learning techniques, specifically artificial neural network surrogate models, and, on the other hand the

capability of 3D interpolation schemes to simulate the time evolution of radiation maps on a fast timescale (around 100 milliseconds to be compliant with the real-time constraints). This simulation is intended to capture the radiation dose rate during maintenance operations in fusion facilities, such as cutting and removing activated pipes for storage in dedicated areas. The ultimate goal is to implement real-time calculations of the nuclear dose rate evolution into virtual reality tools used to simulate, visualize, prepare, and optimize maintenance operations in areas with high dose rates, like those located in the inter-space before the bioshield or in the port-cell behind the bioshield.

Currently, the dose rate assessment in virtual reality tools for fusion applications only deals with static radiation dose rate maps. The new development aims to address more complex situations where the operator can modify the radiation source term, dynamically altering the radiation dose map. The methodology is based on the principles of artificial intelligence, where algorithms are trained to reproduce specific results using a 'learning database' containing data representative of the model. The neural network's learning capability allows to simulate the radiation dose rate based on a database of detailed and precise neutronic Monte-Carlo simulations. As a proof of concept, the methodology focuses on a realistic maintenance scenario of the ITER test blanket module, specifically the European water cooled lithium lead system. The selected maintenance scenario involves disassembling pipes in the pipe-forest of the test blanket module and cutting the front part of pipes into three segments to accommodate a plastic film with an inflated seal that prevents from inter-space and port-cell contamination. However, it should be emphasized that the development and assessment of the methodology are not limited to this specific maintenance scenario. Currently, all the necessary input data (activation data, geometrical data, and radiation map data) for simulating the selected maintenance scenario have been defined. Tools have been developed to prepare various MCNP data files that will be stored in the database for this maintenance scenario. The Uranie platform [117], an open-source framework developed at CEA based on the CERN data analysis platform called ROOT [118], is selected to implement the neural network. The Uranie platform is dedicated to uncertainty propagation, surrogate model development, and optimization issues. In this specific application, it will facilitate the development and training of the neural network using the 'learning' database of neutronic simulations, as well as testing the network's quality with a 'testing' database.

This challenging project was initiated within EUROfusion's work-package PrIO in 2022, and the learning database is currently under construction, incorporating detailed and various neutronic MCNP calculations. Overall, the development of this methodology holds significant potential for enhancing radiation safety during maintenance operations in fusion facilities and may be applied in various maintenance scenarios. The use of artificial intelligence and machine learning techniques as well as the interpolation methods in combination with virtual reality tools opens up exciting possibilities for optimizing worker safety and efficiency in complex and radioactive environments, and, for applying the as low as reasonably achievable methodology as requested by the nuclear regulators.

5. Conclusions

This paper is an overview of the activities performed since early 2021 within a new EUROfusion Work-Package called PrIO. Indeed, in the context of the ITER revised baseline under elaboration by ITER organization [1] and with the aim of achieving $Q = 10$ as soon as possible once the machine construction is complete, it is timely to strengthen our collective effort. This involves ensuring that operational tools, broadly defined to include methods, codes, and sub-systems, are fully tested, validated, and reliable before being transferred to ITER for future scientific exploitation. This paper presents specific examples illustrating the contributions of the EUROfusion Work-Package PrIO in supporting the preparation of ITER's nuclear operations.

Firstly, progress has been made in the development and validation of plasma breakdown and burn-through tools, on synthetic diagnostics for the IR measurement and thermal event detection, for the fast ion loss measurement and the fiber optic current sensors. The objective is to validate tools that can be directly transferred to ITER for the first plasma operation using the common IMAS framework. This represents an initial effort, and further development is planned in the near future. This includes the development of new synthetic diagnostics and integrated data validation. Continuing along the same line of effort, activities have been strengthened in the development and exploitation of multi-machine databases. This is aimed at proposing a rigorous procedure to validate codes using data from various facilities, thereby increasing our confidence in extrapolating to ITER applications. A multi-machine database allows testing algorithms in advance of ITER operation. For example, predicting disruption events with confidence and without triggering unnecessary false alarms.

Secondly, for the ITER heating and current drive subsystems, PrIO is contributing to the development of the RF sources for NBIs and actively participate in the ITER NBTF. The development of the RF source follows a step ladder approach, beginning with sources of different sizes (BATMAN Upgrade, ELISE) before extrapolating to ITER size. These developments have already made unique contributions to the design and operation of the ITER NBTF and the design of ITER NBI system. Examples include long pulse development with reduced co-extracted electrons, Molybdenum (Mo) coating techniques, and RF source optimization. The NBTF, a unique ITER operating test facility, will contribute to the design and operation of the NBI system. Additionally, it provides hands-on training for the new generation of fusion engineers and physics prior to ITER operation.

Finally, ITER will be a nuclear operating fusion facility and in this context multi-year effort has been pursued

within EUROfusion to validate tools and methodology (neutron calibration, neutron measurement) using the unique integrated operation of JET. This effort recently culminated in experiments conducted in 2021 and 2023, involving a mixture of deuterium-tritium fuels with varying tritium levels. Experiments and simulations have been performed to validate in a complex tokamak geometry the methodology and codes to calculate the neutron streaming, shutdown dose rates and neutron induced material radiation effects with exposed ITER materials. The methodology and tools developed are applicable to simulate neutron flux, neutron streaming and neutron-induced material activation for ITER applications. This could include simulations for preparing the two-step nuclear fluence approach recently proposed by the IO [1]. The integrated test performed on JET is crucial for gaining confidence in simulated neutron maps and neutron-induced material activation before extrapolating to larger facilities like ITER or DEMO. The knowledge and nuclear experience acquired is uniquely relevant for the next generation of fusion facilities, taking advantage of its application and validation on JET in a real and complex tokamak geometry with different materials. Thus, the methodology used at JET to precisely validate codes and measurements through dedicated calibration procedures of the 14.1 MeV flux can be directly applied to ITER for its nuclear operations in both deuterium and deuterium–tritium. This work is being extended via two new neutronic experiments implemented during the 2023 JET deuterium–tritium operation to validate codes for calculating the water (flowing in the cooling loops) activation under irradiation by 14.1 MeV neutrons and for estimating the number of neutron-induced events in the electronics components. In the near term, and following the end of JET operation by the end of 2023, efforts on neutronics have been and will be further expanded within PrIO by using the full capability of the existing neutron facilities such as, for instance, at FNG and/or JSI-TRIGA to provide other test beds to validate the nuclear codes (like for predicting the level of ACPs transported in the cooling system) in conditions as closed as possible to the ones expected on nuclear fusion facilities during the various nuclear operating phases.

Acknowledgments

This work has been carried out within the framework of the EUROfusion Consortium, funded by the European Union via the Euratom Research and Training Programme (Grant Agreement No 101052200—EUROfusion). Views and opinions expressed are however those of the author(s) only and do not necessarily reflect those of the European Union or the European Commission. Neither the European Union nor the European Commission can be held responsible for them.

We would like to thank the JET operator (UKAEA) for the continuous support for the implementation of neutronic experiments at JET within PrIO.

This work was partially funded by the Academy of Finland Project Nos. 328874, 353370 and 324759.

Disclaimers

ITER is a Nuclear Facility INB-174. The views and opinions expressed herein do not necessarily reflect those of the ITER Organization.

ORCID iDs

X. Litaudon https://orcid.org/0000-0001-6973-9717
U. Fantz https://orcid.org/0000-0003-2239-3477
V. Toigo https://orcid.org/0000-0002-4925-4752
M.-H. Aumeunier https://orcid.org/0009-0009-6207-5079
J.-L. Autran https://orcid.org/0000-0001-9893-014X
E. Belonohy https://orcid.org/0000-0002-1045-4634
A. Colangeli https://orcid.org/0000-0003-4487-1927
F. Dacquait https://orcid.org/0000-0001-7442-7937
M. Dentan https://orcid.org/0009-0003-2860-3639
M. De Pietri https://orcid.org/0000-0002-2815-6889
J. Eriksson https://orcid.org/0000-0002-0892-3358
M. Fabbri https://orcid.org/0000-0002-9979-3025
L. Figini https://orcid.org/0000-0002-0034-4028
J. Figueiredo https://orcid.org/0000-0003-1356-7666
D. Flammini https://orcid.org/0000-0002-7382-5826
N. Fonnesu https://orcid.org/0000-0002-2800-0040
L. Frassinetti https://orcid.org/0000-0002-9546-4494
J. Galdón-Quiroga https://orcid.org/0000-0002-7415-1894
R. Garcia-Alia https://orcid.org/0000-0001-8030-1804
M. Garcia-Munoz https://orcid.org/0000-0002-3241-502X
J. Gonzalez-Martin https://orcid.org/0000-0002-3237-5195
E. Grelier https://orcid.org/0000-0002-8488-1612
C.L. Grove https://orcid.org/0000-0002-3630-5637
V. Ioannou-Sougleridis https://orcid.org/0000-0002-6478-8330
H.-T. Kim https://orcid.org/0009-0008-2549-5624
L. Kos https://orcid.org/0000-0002-1790-7093
E. Leon-Gutierrez https://orcid.org/0000-0003-4783-2747
A.J. López-Revelles https://orcid.org/0000-0001-7952-2829
D. Marcuzzi https://orcid.org/0000-0001-8341-6586
K.G. Mcclements https://orcid.org/0000-0002-5162-509X
M. Mattei https://orcid.org/0000-0001-7951-6584
K. Mergia https://orcid.org/0000-0002-2633-8750
R. Mitteau https://orcid.org/0000-0003-4708-0151
D. Munteanu https://orcid.org/0000-0003-3672-4433
L.W. Packer https://orcid.org/0000-0003-3539-9587
S. Pamela https://orcid.org/0000-0001-8854-1749
A. Pau https://orcid.org/0000-0002-7122-3346
E. Peluso https://orcid.org/0000-0002-6829-2180
L. Sanchis-Sanchez https://orcid.org/0000-0001-8211-3356
M.I. Savva https://orcid.org/0000-0003-4238-149X
G. Serianni https://orcid.org/0000-0002-4704-2019

A. Snicker https://orcid.org/0000-0001-9604-9666
L. Snoj https://orcid.org/0000-0003-3097-5928
Ž. Štancar https://orcid.org/0000-0002-9608-280X
C. Wimmer https://orcid.org/0000-0003-4691-4265
D. Wünderlich https://orcid.org/0000-0003-2810-9633

References

[1] Barabaschi P. *et al* 2023 Progress on ITER manufacturing, construction, commissioning and plans *29th Fusion Energy Conf.* (*London, UK*, *16–21 October 2023*) [OV/2354]
[2] 2018 European research roadmap to the realisation of fusion energy (available at: www.euro-fusion.org/eurofusion/roadmap/)
[3] Donné A.J.H., Federici G., litaudon X. and Mcdonald D. 2017 *J. Instrum.* **12** C10008
[4] Litaudon X. *et al* 2022 *Plasma Phys. Control. Fusion* **64** 034005
[5] Maggi C. *et al* 2024 *Nucl. Fusion* **64** 112012
[6] King D. *et al* 2024 *Nucl. Fusion* **64**
[7] Mattei M. *et al* 2023 Breakdown studies for JT-60SA: new design tools for ITER operations *29th Fusion Energy Conf.* (*London, UK*, *16–21 October 2023*) [1963]
[8] Yun H.-S. *et al* 2023 Improvement and validation of plasma initiation model for versatile experiment spherical torus *29th Fusion Energy Conf.* (*London, UK*, *16–21 October 2023*) [1906]
[9] Vives S. *et al* 2023 Overview of the final design of the visible and infrared wide angle viewing system diagnostic for ITER in equatorial port 12 *29th Fusion Energy Conf.* (*London, UK*, *16–21 October 2023*) [1835]
[10] Aumeunier M.-H. *et al* 2024 *Nucl. Fusion* **64** 086044
[11] Goussarov A. *et al* 2023 Progress in the development of the fibre optics current sensor for magnetic fusion devices *29th Fusion Energy Conf.* (*London, UK*, *16–21 October 2023*) [1765]
[12] Pau A. *et al* 2023 A modern framework to support disruption studies: the EUROfusion disruption database *29th Fusion Energy Conf.* (*London, UK*, *16–21 October 2023*) [2057]
[13] Fantz U. *et al* 2024 *Nucl. Fusion* **64** 086063
[14] Harder N.D. *et al* 2024 *Nucl. Fusion* **64** 076046
[15] Toigo V. *et al* 2023 Experimental results and plan for the optimisation of the ITER beam injector prototype *29th Fusion Energy Conf.* (*London, UK*, *16–21 October 2023*) [2383]
[16] Packer L.W. *et al* 2023 ITER materials irradiation within the D–T neutron environment at JET: post-irradiation analysis outcomes and recommendations *29th Fusion Energy Conf.* (*London*, *16–21 October 2023*) [1839]
[17] Loughlin M.J. *et al* 2023 Recent developments in radiation transport for fusion reactors and validation of JET DT experiments *29th Fusion Energy Conf.* (*London*, *16–21 October 2023*) [1614]
[18] De Pietri M. *et al* 2023 Development and validation in neutron-irradiated water of FLUNED, an open-source tool for fluid activation calculations *29th Fusion Energy Conf.* (*London*, *16–21 October 2023*) [2096]
[19] Maggi C. *et al* 2023 *Nucl. Fusion* **63** 110201
[20] Batistoni P. *et al* 2014 *Fusion Eng. Des.* **89** 896
[21] Litaudon X. *et al* 2017 *Nucl. Fusion* **57** 102001
[22] Kim H.-T. *et al* 2022 *Nucl. Fusion* **62** 126012
[23] Farina D. 2007 *Fusion Sci. Technol.* **52** 154
[24] Farina D. 2018 *Nucl. Fusion* **58** 066012
[25] Granucci G. *et al* 2015 *Nucl. Fusion* **55** 093025
[26] Di Grazia L.E., Mattei M., Pironti A. and Villone F. 2022 Magnetic control strategies for the breakdown and early ramp-up in large tokamaks *2022 IEEE Conf. on Control Technology and Applications (CCTA)* (*Trieste, Italy*, *2022*) pp 837–44 (available at: https://ccta2022.ieeecss.org/)
[27] Ricci D. *et al* 2019 EC Assisted start-up experiment and predictions for the next generation fusion experiments *Proc. 46th EPS Conf. on Plasma Physics 46th EPS Conf. on Plasma Physics* (*Milan, Italy*, *8–12 July 2019*) p O5.103 (available at: http://ocs.ciemat.es/EPS2019PAP/pdf/O5.103.pdf)
[28] Di Grazia L.E. *et al* 2024 *Nucl. Fusion* **64** 096032
[29] Aumeunier M.-H. *et al* 2021 *Nucl. Mater. Energy* **26** 100879
[30] Aumeunier M.-H., Le Bohec M., Brunet R., Juven A., Adel M., Artusi X., Miorelli R., Reboud C. and Rigollet F. 2022 *Nucl. Mater. Energy* **33** 101231
[31] Aumenier M.-H., Kočan M., Reichle R. and Gauthier E. 2017 *Nucl. Mater. Energy* **12** 1265
[32] Juven A. *et al* 2024 *Nucl. Mater. Energy* **38** 101562
[33] Ben Yaala M., Aumeunier M.-H., Steiner R., Schönenberger M., Martin C., Le Bohec M., Talatizi C., Marot L. and Meyer E. 2021 *Rev. Sci. Instrum.* **92** 093501
[34] Firdaouss M., Riccardo V., Martin V., Arnoux G. and Reux C. 2013 *J. Nucl. Mater.* **438** S536
[35] Kos L., Pitts R.A., Simič G., Brank M., Anand H. and Arter W. 2019 *Fusion Eng. Des.* **146** 1796
[36] Mitteau R., Belafdil C., Balorin C., Courtois X., Moncada V., Nouailletas R. and Santraine B. 2021 *Fus. Eng. Des.* **165** 112223
[37] Grelier E., Mitteau R. and Moncada V. 2022 *Plasma Phys. Control. Fusion* **64** 104010
[38] Grelier E., Mitteau R. and Moncada V. 2023 *Fusion Eng. Des.* **192** 113636
[39] Quercia A., Pironti A., Bolshakova I., Holyaka R., Duran I. and Murari A. (JET Contributors) 2022 *Nucl. Fusion* **62** 106032
[40] Moreau P.H., Brichard B., Fil A., Malard P., Pastor P., Le-Luyer A., Samaille F. and Massaut V. 2011 *Fusion Eng. Des.* **86** 1222
[41] Gusarov A., Leysen W., Beaumont P., Wuilpart M., Dandu P., Boboc A., Croft D., Bekris N. and Batistoni P. 2021 *Fusion Eng. Des.* **165** 112228
[42] Galdon-Quiroga J. *et al* 2018 *Nucl. Fusion* **58** 036005
[43] Zweben S.J. 1989 *Nucl. Fusion* **29** 825–33
[44] García-Muñoz M., Fahrbach H.-U. and Zohm H. 2009 *Rev. Sci. Instrum.* **80** 053503
[45] Garcia-Munoz M. *et al* 2016 *Rev. Sci. Instrum.* **87** 11D829
[46] Gonzalez-Martin J. *et al* 2019 *J. Instrum.* **14** C11005
[47] Gonzalez-Martin J. *et al* 2018 *Rev. Sci. Instrum.* **89** 10I106
[48] Rivero-Rodriguez J.F. *et al* 2018 *Rev. Sci. Instrum.* **89** 10I112
[49] Ayllon-Guerola J. *et al* 2021 *Fusion Eng. Des.* **167** 112304
[50] Hirvijoki E., Asunta O., Koskela T., Kurki-Suonio T., Miettunen J., Sipilä S., Snicker A. and Äkäslompolo S. 2014 *Comput. Phys. Commun.* **185** 1310
[51] Sipilä S. *et al* 2021 *Nucl. Fusion* **61** 086026
[52] Sanchis L. *et al* 2019 *Plasma Phys. Control. Fusion* **61** 014038
[53] Gonzalez-Martin J. *et al* 2021 *Rev. Sci. Instrum.* **92** 053538
[54] Galdon-Quiroga J. *et al* 2018 *Plasma Phys. Control. Fusion* **60** 105005
[55] Frassinetti L. *et al* 2021 *Nucl. Fusion* **61** 016001
[56] Gillgren A., Fransson E., Yadykin D., Frassinetti L., Strand P. and Contributors J. 2002 *Nucl. Fusion* **62** 096006
[57] Kit A., Järvinen A.E., Wiesen S., Poels Y. and Frassinetti L. 2023 *Nucl. Mater. Energy* **34** 101347

[58] Pau A., Fanni A., Carcangiu S., Cannas B., Sias G., Murari A. and Rimini F. 2019 *Nucl. Fusion* **59** 106017
[59] Giacomin M., Pau A., Ricci P., Sauter O. and Eich T. (the ASDEX Upgrade team, JET Contributors and the TCV team) 2022 *Phys. Rev. Lett.* **128** 185003
[60] Toigo V. *et al* 2017 *Nucl. Fusion* **57** 086027
[61] Marcuzzi D. *et al* 2023 *Fusion Eng. Des.* **191** 113590
[62] Ichikawa M. *et al* 2023 Progress of electrical and nuclear safety design of DC 1 MV power supply system for the ITER neutral beam injector *29th Fusion Energy Conf.* (*London, UK*, *16–21 October 2023*) [1644]
[63] Tobari H. *et al* 2023 Progress on long-pulse and ITER-relevant-intensity negative ion beam accelerations for ITER neutral beam injector *29th Fusion Energy Conf.* (*London, UK*, *16–21 October 2023*) [1691]
[64] Pandya K. *et al* 2024 *J. Instrum.* **19** C02020
[65] Fantz U. *et al* 2022 Ion source developments at IPP: on the road towards achieving the ITER-NBI targets and preparing concepts for DEMO *J. Phys.: Conf. Ser.* **2244** 012049
[66] Wünderlich D., Wimmer C., Riedl R., Bonomo F., Fröschle M., Mario I., Mimo A., Yordanov D., Fantz U. and Heinemann B. 2021 NNBI for ITER: status of long pulses in deuterium at the test facilities BATMAN upgrade and ELISE *Nucl. Fusion* **61** 096023
[67] Fantz U. *et al* 2023 RF-driven ion sources for neutral beam injectors for fusion devices *Physics and Applications of Hydrogen Negative Ion Sources* (*Springer Series on Atomic, Optical, and Plasma Physics*) vol 124, ed M. Bacal (Springer)
[68] Fantz U., Bonomo F., Fröschle M., Heinemann B., Hurlbatt A., Kraus W., Schiesko L., Nocentini R., Riedl R. and Wimmer C. 2019 *Fusion Eng. Des.* **146** 212
[69] Belonohy E. *et al* 2022 Operations knowledge management in the EUROfusion operations network *32nd Symp. on Fusion Technology* (*Dubrovnik, Croatia*, *18–23 September 2022*) (https://doi.org/10.1063/1.4962809)
[70] Peglau M. *et al* 2023 *Fusion Eng. Des.* **189** 113382
[71] Nocentini R., Heinemann B. and Hurlbatt A. 2023 *Fusion Eng. Des.* **190** 113504
[72] Mimo A., Wimmer C., Wünderlich D. and Fantz U. 2018 Studies of Cs dynamics in large ion sources using the CsFlow3D code *AIP Conf. Proc.* **2052** 040009
[73] Serianni G. *et al* 2020 *Rev. Sci. Instrum.* **91** 023510
[74] Sartori E. *et al* 2022 *Nucl. Fusion* **62** 086022
[75] serianni G. *et al* 2023 *IEEE Trans. Plasma Sci.* **51** 927
[76] Veltri P. *et al* 2022 Towards low divergence beams for the ITER neutral beam injection system *8th Int. Symp. on Negative Ions, Beams and Sources* (*Padova, Italy*, *2–7 October 2022*) (available at: https://indico.cern.ch/event/1098715/timetable/?view=standard_numbered)
[77] Serianni G. *et al* 2022 *Rev. Sci. Instrum.* **93** 081101
[78] Shepherd A., Pouradier-Duteil B., Patton T., Pimazzoni A., Garola A.R., Sartori E. and Serianni G. 2022 *IEEE Trans. Plasma Sci.* **50** 3906
[79] Shepherd A. *et al* 2023 *J. Inst.* **18** C07019
[80] Chitarin G. *et al* 2022 *IEEE Trans. Plasma Sci.* **50** 2755
[81] Schneider M., Lerche E., Van Eester D., Hoenen O., Jonsson T., Mitterauer V., Pinches S.D., Polevoi A.R., Poli E. and Reich M. 2021 *Nucl. Fusion* **61** 126058
[82] Zohar A. *et al* 2021 *Fusion Eng. Des.* **163** 112158
[83] Villari R. *et al* 2022 Neutronics, nuclear waste and safety activities within EUROfusion in support of preparation of ITER operations *32nd Symp. on Fusion Technology* (*Dubrovnik, Croatia*, *18–23 September 2022*) [IP-5.1] (available at: https://soft2022.eu/)
[84] Batistoni P., Conroy S., Lilley S., Naish J., Obryk B., Popovichev S., Stamatelatos I., Syme B. and Vasilopoulou T. 2015 *Nucl. Fusion* **55** 053028
[85] Fonnesu N., Villari R., Flammini D., Batistoni P., Fischer U. and Pereslavtsev P. 2020 *Fusion Eng. Des.* **161** 112009
[86] Villari R. *et al* 2017 *Fusion Eng. Des.* **123** 171
[87] Villari R. *et al* 2018 *Fusion Eng. Des.* **136** 1545
[88] Kos B., Mosher S.W., Kodeli I.A., Grove R.E., Naish J., Obryk B., Villari R. and Batistoni P. 2019 *Fusion Eng. Des.* **147** 111252
[89] Naish J., Batistoni P., Kos B., Obryk B., Villari R., Vasilopoulou T. and Stamatelatos I.E. 2021 *Fusion Eng. Des.* **170** 112538
[90] Kos B., Radulescu G., Grove R., Villari R. and Batistoni P. 2023 *Fusion Sci. Technol.* **79** 284
[91] Batistoni P., Angelone M., Fischer U., Klix A., Kodeli I., Leichtle D., Pillon M., Pohorecki W. and Villari R. 2012 *Nucl. Fusion* **52** 083014
[92] Villari R. *et al* 2023 Key technological aspects of recent DT operations at JET *Invited Talk at 15th Int. Symp. on Fusion Nuclear Technology* (*Spain*, *10–15 September 2023*) (available at: https://isfnt2023.com/)
[93] Andreoli F. *et al* 2020 *EPJ WEB Conf.* **239** 21002
[94] Villari R., NAgy D., Bertalot L., Colangeli A., Flammini D., Fonnesu N., Mariano G., Moro F. and Polunovskiy E. 2022 *IEEE Trans. Plasma Sci.* **11** 4533
[95] Angelone M., Fonnesu N., Colangeli A., Moro F., Pillon M. and Villari R. 2019 *Fusion Eng. Des.* **146** 1755
[96] Packer L.W. *et al* 2021 *Nucl. Fusion* **61** 116057
[97] Packer L.W. *et al* 2018 *Nucl. Fusion* **58** 096013
[98] Batistoni P.R. *et al* 2018 *Radiat. Prot. Dosim.* **180** 102
[99] Sublet J.-C., Eastwood J.W., Morgan J.G., Gilbert M.R., Fleming M. and Arter W. 2017 *Nucl. Data Sheets* **139** 77
[100] Autran J.L. *et al* 2022 *IEEE Trans. Nucl. Sci.* **69** 501
[101] Dentan M. *et al* 2022 Preliminary study of electronics reliability in ITER neutron environment *European Workshop on Radiation and its Effects on Components and Systems (RADECS 2022)* (*Venise, Italy*, *October 2022*) p hal–03735989 (available at: https://radecs2022.dei.unipd.it/)
[102] Cecchetto M., Alia R.G., Wrobel F., Coronetti A., Bilko K., Lucsanyi D., Fiore S., Bazzano G., Pirovano E. and Nolte R. 2021 *IEEE Trans. Nucl. Sci.* **68** 873
[103] Loughlin M., Angelone M., Batistoni P., Bertalot L., Eskhult J., Konno C., Pampin R., Polevoi A. and Polunovskiy E. 2014 *Fusion Eng. Des.* **89** 1865
[104] Batistoni P., Fischer U., Ochiai K., Petrizzi L., Seidel K. and Youssef M. 2008 *Fusion Eng. Des.* **83** 834
[105] Žohar A., Lengar I. and Snoj L. 2020 *Fusion Eng. Des.* **160** 111828
[106] De Pietri M., Alguacil J., Rodríguez E. and Juárez R. 2023 *Comput. Phys. Commun.* **291** 108807
[107] Angelone M., Pillon M., Loreti S., Colangeli A., Mazzitelli G., Del Prete P., Villari R., Naish J., Nobs C.R. and Packer L.W. 2020 *Fusion Eng. Des.* **160** 111998
[108] Radulovic V., Rupnik S., Naish J., Bradnam S., Ghani Z., Popovichev S., Kiptily V., Batistoni P., Villari R. and Snoj L. 2021 *Fusion Eng. Des.* **169** 112410
[109] Kotnik D., Basavaraj A.K., Snoj L. and Lengar I. 2023 *Fusion Eng. Des.* **193** 113632
[110] Pampin R., Cau F. and Pampin R. 2022 *Fusion Eng. Des.* **181** 113171
[111] Chiovaro P., Ciattaglia S., Cismondi F., Del Nevo A., Di Maio P.A., Federici G., Frittitta C., Moscato I., Spagnuolo G.A. and Vallone E. 2020 *Fusion Eng. Des.* **157** 111697

[112] Pampin R. *et al* 2024 *Fusion Eng. Des.* **204** 114466 (available at: www.sciencedirect.com/science/article/pii/S0920379624003193)
[113] Berry T.A., Nobs C.R., Dubas A., Worrall R., Eade T., Naish J. and Packer L.W. 2021 *Fusion Eng. Des.* **173** 112894
[114] Nobs C.R., Naish J., Packer L.W., Worrall R., Angelone M., Colangeli A., Loreti S., Pillon M. and Villari R. 2020 *Fusion Eng. Des.* **159** 111743
[115] Dacquait F. *et al* 2020 Modelling of the contamination transfer in nuclear reactors: the OSCAR code applications to sodium-cooled fast reactors and ITER *1st IAEA Workshop on Challenges for Coolants in Fast Neutron Spectrum Systems* (*Vienna (Austria)*, *5–7 July 2017*) p TECDOC–1912 (available at: www-pub.iaea.org/MTCD/Publications/PDF/TE-1912_web.pdf)
[116] Dacquait F., Francescatto J., Tevissen E., Genin J.-B., You D., Cherpin C. and Broutin F. 2023 *Nucl. Eng. Des.* **405** 112190
[117] Blanchard J.B., Damblin G., Martinez J.-M., Arnaud G. and Gaudier F. 2019 *EPJ Nucl. Sci. Technol.* **5** 4
[118] ROOT: analyzing petabytes of data, scientifically. An open-source data analysis framework used by high energy physics and others (available at: https://root.cern.ch)